การตรึงเอนไซม์ไลเพสจาก *Candida rugosa* ลงบนคาร์บอนโมโนลิทที่มีรูพรุนแบบลำดับขั้น

นายบดินทร์ เหลืองอ่อน

ศูนย์วิทยทรัพยากร
จุฬาลงกรณ์มหาวิทยาลัย

วิทยานิพนธ์นี้เป็นส่วนหนึ่งของการศึกษาตามหลักสูตรปริญญาวิศวกรรมศาสตรมหาบัณฑิต
สาขาวิชาวิศวกรรมเคมี ภาควิชาวิศวกรรมเคมี
คณะวิศวกรรมศาสตร์ จุฬาลงกรณ์มหาวิทยาลัย
ปีการศึกษา 2552

ลิขสิทธิ์ของจุฬาลงกรณ์มหาวิทยาลัย

IMMOBILIZATION OF *Candida rugosa* LIPASE ON HIERARCHICAL POROUS CARBON MONOLITH

Mr. Bordin Luangon

ศูนย์วิทยทรัพยากร
จุฬาลงกรณ์มหาวิทยาลัย

A Thesis Submitted in Partial Fulfillment of the Requirements
for the Degree of Master of Engineering Program in Chemical Engineering
Department of Chemical Engineering
Faculty of Engineering
Chulalongkorn University
Academic Year 2009
Copyright of Chulalongkorn University

Thesis Title	IMMOBILIZATION OF *Candida rugosa* LIPASE ON HIERARCHICAL POROUS CARBON MONOLITH
By	Mr. Bordin Luangon
Field of Study	Chemical Engineering
Thesis Advisor	Assistant Professor Nattaporn Tonanon, D.Eng
Thesis Co-Advisor	Adisak Siyasukh, D.Eng
Thesis Co-Advisor	Pakorn Winayanuwattikun, Ph.D.

Accepted by the Faculty of Engineering, Chulalongkorn University in Partial Fulfillment of the Requirements for the Master's Degree

..... Dean of the Faculty of Engineering
(Associate Professor Boonsom Lerdhirunwong, Dr.Ing.)

THESIS COMMITTEE

..... Chairman
(Associate Professor Sarawut Rimdusit, Ph.D.)

..... Thesis Advisor
(Assistant Professor Nattaporn Tonanon, D.Eng.)

..... Thesis Co-Advisor
(Adisak Siyasukh, D.Eng)

..... Thesis Co-Advisor
(Pakorn Winayanuwattikun, Ph.D.)

..... Examiner
(Assistant Professor Varong Pavarajarn, Ph.D.)

..... External Examiner
(Sorapong Pavasupree, Ph.D.)

บดินทร์ เหลืองอ่อน : การตรึงเอนไซม์ไลเพสจาก *Candida rugosa* ลงบนคาร์บอนโมโนลิทที่มีรูพรุนแบบลำดับขั้น (IMMOBILIZATION OF *Candida rugosa* LIPASE ON HIERARCHICAL POROUS CARBON MONOLITH) อาจารย์ที่ปรึกษาวิทยานิพนธ์หลัก: ผศ.ดร.ณัฐพร โทณานนท์, อาจารย์ที่ปรึกษาวิทยานิพนธ์ร่วม: อ.ดร.อดิศักดิ์ ไสยสุข และอ.ดร.ปกรณ์ วินะยานุวัติคุณ, 68 หน้า.

งานวิจัยนี้เป็นการศึกษาการตรึงเอนไซม์ไลเพสจาก *Candida rugosa* ลงบนคาร์บอนโมโนลิทที่มีรูพรุนแบบลำดับขั้น โดยคาร์บอนโมโนลิทที่ใช้จะสังเคราะห์มาจากรีโซซินอล-ฟอร์มัลดีไฮด์ (อาร์-เอฟ) เจล ผ่านกระบวนการคาร์บอไนเซชั่น ซึ่งจะได้คาร์บอนโมโนลิทที่ไม่มีออกซิเจนอยู่บนพื้นผิว และกระบวนการกระตุ้นเชิงความร้อน ซึ่งจะได้คาร์บอนโมโนลิทที่มีออกซิเจนอยู่บนพื้นผิว คาร์บอนที่ได้จากทั้งสองกระบวนการนี้จะมีรูพรุน และพื้นที่ผิวสูง จึงเหมาะที่จะนำมาใช้ในการตรึงเอนไซม์ ในงานวิจัยนี้จะนำคาร์บอนทั้งสองชนิดนี้มาตรึงเอนไซม์ไลเพส ใช้วิธีการดูดซับเชิงกายภาพ โดยการป้อนสารละลายเอนไซม์ไหลวนผ่านคาร์บอนโมโนลิทที่บรรจุอยู่ในคอลัมน์ และเพื่อเป็นการประหยัด และลดปริมาณของเอนไซม์ จะใช้คาร์บอนที่มีลักษณะเป็นเม็ด ซึ่งมีลักษณะเชิงกายภาพเหมือนกับคาร์บอนโมโนลิทมาช่วยในการหาสภาวะเบื้องต้น (pH, ความเข้มข้นของสารละลายบัฟเฟอร์ และความเข้มข้นของสารละลายเอนไซม์) ที่เหมาะสมในการเตรียมสารละลายเอนไซม์ก่อนจะตรึงเอนไซม์ผ่านคอลัมน์ ค่า pH, ความเข้มข้นของสารละลายบัฟเฟอร์ และความเข้มข้นของเอนไซม์ที่เหมาะสมที่ได้ มีค่าเท่ากับ 7, 20 มิลลิโมล และ 1 มิลลิกรัมต่อมิลลิลิตร ตามลำดับ ในส่วนของการตรึงเอนไซม์ผ่านคอลัมน์ ผลที่ได้ชี้ให้เห็นว่าเวลาที่ใช้ในการตรึงเอนไซม์จะสั้นมาก ซึ่งอาจจะเป็นผลมาจากการใช้วิธีการป้อนสารละลายเอนไซม์เข้าไปในคอลัมน์ ทำให้เอนไซม์สามารถเข้าถึงโครงสร้างภายในของคอลัมน์ได้มากขึ้น และดีขึ้นด้วย ช่วยเพิ่มประสิทธิภาพในการตรึงเอนไซม์ นอกจากนั้นแล้วอัตราการไหลของสารละลายเอนไซม์ที่ใช้ในการตรึงก็ยังมีผลต่อเอนไซม์ กล่าวคือยิ่งอัตราการไหลมีค่ามาก ประสิทธิภาพของเอนไซม์ก็จะมากขึ้นตามไปด้วย ซึ่งอาจจะเป็นผลมาจากที่อัตราการไหลมีค่าสูง ช่วยให้เอนไซม์สามารถกระจายตัวบนพื้นผิวของคาร์บอนได้ดีขึ้น เป็นผลให้ประสิทธิภาพของเอนไซม์มีค่าสูงขึ้น ส่วนพฤติกรรมของเอนไซม์ที่ถูกตรึงบนคาร์บอนโมโนลิทที่มีออกซิเจนอยู่บนพื้นผิว และไม่มีออกซิเจนบนพื้นผิว จะมีพฤติกรรมการเกิดปฏิกิริยาที่แตกต่างกัน โดยคาร์บอนที่มีออกซิเจนอยู่บนพื้นผิว การเกิดปฏิกิริยาของเอนไซม์จะเป็นไปตามสมการของ Michaelis-Menten เหมือนกับลักษณะของเอนไซม์ทั่วไป ส่วนเอนไซม์ที่ถูกตรึงอยู่บนคาร์บอนที่ไม่มีออกซิเจนอยู่บนพื้นผิว ได้แสดงลักษณะแบบ sigmoidal ซึ่งอาจจะเกิดจากขีดจำกัดของการละลายของซับสเตรต และค่า K' ของคอลัมน์ที่บรรจุคาร์บอนโมโนลิทที่ไม่มีออกซิเจนอยู่บนพื้นผิว มีค่าน้อยกว่าค่า K_m ของคอลัมน์ที่บรรจุคาร์บอนโมโนลิทที่มีออกซิเจน แสดงว่าคอลัมน์ที่บรรจุแท่งคาร์บอนโมโนลิทที่ไม่มีออกซิเจนอยู่บนพื้นผิวมีประสิทธิภาพน้อยกว่าคอลัมน์ที่บรรจุคาร์บอนโมโนลิทที่มีออกซิเจนอยู่บนพื้นผิว นอกจากนั้นแล้วยังพบว่า ออกซิเจนที่อยู่บนพื้นผิวของคาร์บอนโมโนลิทยังช่วยเพิ่มความสามารถในการตรึงให้มีค่ามากขึ้นด้วย

ภาควิชา.....วิศวกรรมเคมี..... ลายมือชื่อนิสิต.....บดินทร์ เหลืองอ่อน.....

สาขาวิชา.....วิศวกรรมเคมี..... ลายมือชื่อ อ.ที่ปรึกษาวิทยานิพนธ์หลัก.....

ปีการศึกษา.....2552..... ลายมือชื่อ อ.ที่ปรึกษาวิทยานิพนธ์ร่วม.....

ลายมือชื่อ อ.ที่ปรึกษาวิทยานิพนธ์ร่วม.....

5170583521 : MAJOR CHEICAL ENGINEERING
KEYWORDS : IMMOBILIZED LIPASE / HIERARCHICAL / CARBON MONOLITH / RF GEL

BORDIN LUANGON: IMMOBILIZATION OF *Candida rugosa* LIPASE ON HIERARCHICAL POROUS CARBON MONOLITH. THESIS ADVISOR: ASST. PROF. NATTAPORN TONANON, D.Eng, THESIS CO-ADVISOR: ADISAK SIYASUKH, D.Eng. AND PAKORN WINAYANUWUTTIKUN, Ph.D., 68 pp.

Candida rugosa lipase is immobilized into the column packed hierarchical porous carbon monolith. The carbon monolith is synthesized from resorcinol-formaldehyde (RF) gels by sol-gel polycondensation. The surface of carbon monoliths with (C-CO_2) and without (C-N_2) oxygen are obtained by thermal activation and carbonization, respectively. Physical adsorption by recirculation of enzyme solution is applied as immobilization technique. The carbon bead is also used as a support to study the optimal primary conditions (pH, ionic strength and protein loading). The optimal pH and ionic strength are obtained at 7 and 20 mM, respectively as a result of more protein binding ratio. However, optimal protein loading (1 mg/ml) shows the high lipase activity, while the protein binding ratio is low therefore there is a high possibility that all lipase on the support cannot fully work. Moreover, the effects of steric impediments and the enzyme distributions on the support are also significant. The short immobilization time of lipase on hierarchical porous carbon monolith indicates that enzymes rapidly fill the pores and attach on the surface of the porous carbon which result in rapid decrease in residual activity. Moreover, at low flow rate of enzyme solution the protein binding ratio can be improved because enzyme has more time to attach not only to enzyme and support, but also to enzyme and enzyme binding, whereas the lipase activity is low since the steric impediment and low enzyme distribution. For the kinetic behaviors of immobilized enzyme in the column, it is obviously seen that immobilization of lipase on different functional group surface support can change the reaction mechanism of enzyme. In case of immobilized enzyme in C-CO_2 column show the basic general enzyme-catalyzed reaction followed by Michaelis-Menten equation while immobilized enzyme in C-N_2 column show enzyme kinetic like a sigmoidal curve which might be cause from the solubility limit of the polar substrate in hydrophobic solvent. The C-N_2 column kinetic, K'' is lower than K_m from C-CO_2 column which this result indicates that C-N_2 column is less effective than C-CO_2 column. Furthermore, oxygenated surface of C-CO_2 column can help to improve more protein binding ratio.

Department.....Chemical Engineering.....	Student's Signature Bordin Luangon
Field of Study.....Chemical Engineering.....	Advisor's Signature
Academic Year...2009.....	Co-Advisor's Signature A. Siyasukh
	Co-Advisor's Signature Pakorn Winayanuwattikun

ACKNOWLEDGEMENTS

I would like to express my deepest appreciation to my advisor, Assistant Professor Nattaporn Tonanon, D.Eng, for her constant supervision, encourage, and kindly support throughout the course of this thesis. Without her sincere help and enlightening advices, this work must not be achieved.

I would like to express my gratitude to my co-advisors, Adisuk Siyasukh, D.Eng, and Pakorn Winayanuwattikun, Ph.D, for their great advices and useful comments throughout all experiment in this research.

I would like to acknowledge Associate Professor Sarawut Rimdusit, Ph.D, Assistant Professor Varong Pavarajarn, Ph.D, and Sorapong Pavasupree, Ph.D, for their useful comments and participation as the thesis committees.

I would like to acknowledge Miss Kingkeaw Piriyakananon and graduate students at Department of Biotechnology, Faculty of Science, Chulalongkorn University, for their kindly helping and facilities in the lipase immobilization. Moreover, I would like to thanks Department of Biotechnology, Faculty of Science, Chulalongkorn University, for facilitative supports and laboratory space on my work.

I would like to thanks all friends and staffs in Center of Excellence in Particle Technology (CEPT), at Department of Chemical Engineering, Chulalongkorn University, for their supporting and kind assistance.

This work has been fully supported by Chulalongkorn University Centenary Academic Development Project.

Finally, I would like to close with my deepest appreciation to my family and Miss Pariyanee Chongchoho for their understanding, assistance, constant encouragement and warmhearted support throughout my entire education.

CONTENTS

PAGE

ABSTRACT (IN THAI)..... iv
ABSTRACT (IN ENGLISH)..... v
ACKNOWLEDGEMENTS..... vi
CONTENTS..... vii
LIST OF TABLES..... x
LIST OF FIGURES..... xi
NOMENCLATURES..... xiii

CHAPTER I
INTRODUCTION..... 1
1.1 Introduction..... 1
1.2 Objective of this research..... 2
1.3 Scope of work..... 3

CHAPTER II THEORETICAL BACKGROUND AND LITERATURE REVIEWS.....5
2.1 Hierarchical porous carbon monolith..... 5
2.1.1 Resorcinol-formaldehyde gels.....5
2.1.2 Synthesis of RF gels and carbon gels.....5
2.1.3 Application of hierarchical porous carbon monolith gels..... 8
2.2 Lipase.....9
2.2.1 *Candida rugosa* lipase.....9
2.2.2 Enzymatic reaction of lipase..... 10
2.2.3 Applications of lipase.....11
2.3 Immobilization of enzyme.....11
2.3.1 Immobilization methods.....13
2.3.2 Review papers for Immobilization of enzyme..... 15

PAGE

CHAPTER III EXPERIMENTAL PROCEDURE..... 17
3.1 Chemical reagents.....17
3.2 Equipments..... 18
3.2.1 Basic equipments.....18
3.2.2 Column reactor apparatus..... 19
3.3 Characterizations..... 20
3.4 Experimental procedures..... 20
3.4.1 Preparation of the carbon bead and monolith supports.....20
3.4.1.1 Preparation of RF solutions..... 21
3.4.1.2 Formation of macroporous carbon beads.....22
3.4.1.3 Formation of macroporous carbon monoliths containing various pore characteristics.....22
3.4.2 The optimization conditions for lipase immobilization.....24
3.4.2.1 Preparation of lipase immobilization on macro porous carbon beads.....24
3.4.2.2 Enzyme activity assay for immobilized carbon beads.....24
3.4.2.3 Protein assay..... 25
3.4.3 Immobilization of lipase on hierarchical porous carbon monoliths using enzyme circulation method..... 25
3.4.3.1 Packing of carbon monolith in the column.....25
3.4.3.2 Immobilization of lipase on a column containing hierarchical porous carbon monolith.....26
3.4.3.3 Enzyme activity assays for immobilized carbon monolith..... 26

CHAPTER IV RESULTS AND DISCUSSIONS..... 27
4.1 Characterizations of carbon supports.....27
4.1.1 Characterization of macroporous carbon beads.....27
4.1.1.1 Structure of carbon beads..... 27
4.1.1.2 Porous properties of RF and carbon beads..... 29

PAGE

4.1.2 Characterization of carbon monoliths..... 29
4.1.2.1 Structure of RF and carbon monoliths.....29
4.1.2.2 Porous properties of RF and carbon monoliths..... 31
4.1.2.3 Oxygenated functional groups on surface of RF and carbon monoliths.....33
4.2 Optimal conditions for lipase immobilization on carbon RF gels..... 37
4.2.1 The effect of pH on immobilization.....37
4.2.2 The effect of ionic strength on immobilization..... 38
4.2.3 The effect of protein loading on immobilization.....39
4.3 Immobilization of *Candida rugosa* lipase on hierarchical porous carbon monoliths..... 40
4.3.1 The effect of immobilization times on residual activity of lipase.....40
4.3.2 The effect of flow rate on immobilization of lipase.....41
4.3.3 Kinetic parameter of column packed hierarchical porous carbon monolith..... 42

CHAPTER V CONCLUSIONS..... 45
5.1 Properties of carbon supports.....45
5.2 Optimal conditions of lipase immobilization..... 45
5.3 The immobilization of lipase on column packed carbon monolith supports..... 46

REFERENCES.....48

APPENDICES.....53
Appendix A Properties of supports.....54
Appendix B Hydrolysis assays..... 63
Appendix C Protein determination..... 64
Appendix D Calculation of the lipase activity.....65
BIOGRAPHY.....68

LIST OF TABLES

PAGE

Table 2.1 Selected characteristic parameters of immobilized enzymes..... 12
Table 2.2 Comparison of each enzyme immobilization techniques..... 14
Table 3.1 List of chemical reagents in this research..... 19
Table 4.1 Physical properties of RF and carbon monoliths..... 30
Table 4.2 Porosity of carbon monoliths..... 31
Table 4.3 Infrared spectrum peaks for an interpretation of surface functional groups.....33
Table 4.4 Kinetic parameter of carbon monoliths.....42
Table A-1 Pore size distribution by volume of C-CO_2..... 54
Table A-2 Pore size distribution by volume of C-N_2..... 57
Table A-3 Size distribution by volume of C-N_2.....60
Table A-4 N_2 Adsorption-Desorption Isotherm at 77K of C-CO_2 monolith.....61
Table A-5 N_2 Adsorption-Desorption Isotherm at 77K of C-N_2 monolith..... 62
Table D-1 Composition for standard BSA..... 65

ศูนย์วิทยทรัพยากร
จุฬาลงกรณ์มหาวิทยาลัย

LIST OF FIGURES

PAGE

Figure 1.1 Schematic diagrams of the scopes in this work.....3

Figure 2.1 Reaction mechanism of the sol-gel polymerization of resorcinol with formaldehyde.....6

Figure 2.2 Schematic diagram of the sol-gel polycondensation of a RF solution.....6

Figure 2.3 Structure formation during the sol-gel transition..... 7

Figure 2.4 Structure of *Candida rugosa* lipase.....10

Figure 2.5 Classification of immobilization methods.....13

Figure 3.1 Illustration of column reactor set up for step of enzyme immobilization and activity assays..... 19

Figure 3.2 Preparation of carbon beads and carbon monolith diagrams.....21

Figure 3.3 Diagram of the furnace system.....23

Figure 3.4 Cross section of the column.....25

Figure 4.1 Photograph of RF and carbon beads..... 27

Figure 4.2 SEM micrograph of carbon beads.....28

Figure 4.3 Particle size distribution of carbon bead..... 28

Figure 4.4 N_2 adsorption-desorption isotherm of macroporous carbon bead..... 29

Figure 4.5 Photograph of RF and carbon monoliths.....30

Figure 4.6 The SEM images show the cross-section of RF monolith gels.....30

Figure 4.7a The SEM images show the cross-section of C-N_2..... 31

Figure 4.7b The SEM images show the cross-section of C- CO_2.....31

Figure 4.8 The macropore size distributions of C-N_2 and C-CO_2..... 32

Figure 4.9 The N_2 adsorption-desorption isotherms of the C-N_2 and C-CO_2.....32

Figure 4.10a FTIR spectra of the RF monolith..... 35

Figure 4.10b FTIR spectra of the carbon monolith obtained from thermal activation..... 35

Figure 4.10c FTIR spectra of the carbon monolith obtained from carbonization... 35

PAGE

Figure 4.11 Possibly oxygenated function group of the carbon monolith prepared by thermal activation.....37

Figure 4.12 The effect of pH on the lipase activity and activity yield (%) of lipase immobilization at 20mM ionic strength and 3 mg/ml protein loading..... 37

Figure 4.13 The effect of ionic strength on the lipase activity and activity yield (%) of lipase immobilization at pH 7 and 3 mg/ml protein loading..... 38

Figure 4.14 The effect of protein loading on the lipase activity and activity yield (%) of lipase immobilization at pH 7 and 20mM ionic strength.....39

Figure 4.15 Residual activities at various immobilization times.....40

Figure 4.16 The effect of flow rate at recirculation of lipase solution in immobilization process on cumulative product at various reaction time.....41

Figure 4.17 The kinetic behavior and parameters of C-CO_2 and C-N_2 column followed by Michaelis-Menten and Boltzmann sigmoidal equations, respectively..... 43

Figure D-1. Calibration curve for protein determination by Bradford's method.....66

ศูนย์วิทยทรัพยากร
จุฬาลงกรณ์มหาวิทยาลัย

NOMENCLATURES

C/W = Mole to volume ratio of catalyst to water [mol/m^3]

$Ca(NO_3)_2$ = Calcium nitrate

CO_2 = Carbon dioxide gas

dp = Macropore size [μm]

et al. = et alibi (latin), and others

F = Formaldehyde

FT-IR = Fourier Transform Infrared Spectroscopy

K_m = Kinetic constant for Michaelis-Menten equation

K'' = Kinetic constant for Boltzmann sigmoidal equation

M = Molar [mol/liter]

mM = Millimolar

μmol = Micromole

μl = Microliter

nm = Nanomater

N_2 = Nitrogen gas

P/P_0 = Relative pressure of N_2 gas [-]

R = Resorcinol

R/F = Molar ratio of resorcinol to formaldehyde [-]

R/W = Molar ratio of resorcinol to de-ionized water [-]

RF = Resorcinol-formaldehyde gel

S_{BET} = Specific surface area determined by BET model [m^2/g]

SEM = Scanning electron microscopy

S_{sp} = Specific surface area determined by average from S_{BET} and $S_{t\text{-}plot}$ [m^2/g]

STP = Standard temperature (0 ºC) and pressure (1 atm)

$S_{t\text{-}plot}$ = Specific surface area determined by t-plot model [m^2/g]

V = Adsorption volume at STP of N_2 [cm^3/g]

V_{macro} = Macropore volume [cm3/g]

V_{max} = Maximum velocity of reaction

V_{micro} = Micropore volume [cm^3/g]

v/v = Volume by volumn

W = De-ionized water

w/w = Weight by weight

ศูนย์วิทยทรัพยากร
จุฬาลงกรณ์มหาวิทยาลัย

CHAPTER I

INTRODUCTION

1.1 Introduction

Immobilizations of free enzyme onto solid supports have been developed to improve the enzyme properties. Since, the enzyme is an effective biocatalyst that increases the rate of reaction and has high substrate specificity, but the separations of enzyme from the product are necessary. The immobilizations of enzyme are the best choice to solve this problem which leads to ease of product and enzyme separation. Although, the activity of immobilized enzyme usually decreases slightly upon immobilization process, they possess important advantages over the improvement of the biocatalyst stability and reusability for application in continuous system with a positive economy on the process. Several of enzyme immobilization techniques have been used, such as an encapsulation, covalent attachment, ionic interaction and physical absorption. The adsorption technique is considered as a simple method because it is easy to be applied and low cost operation, but the binding forces enzyme-support are often weak and leaching of the enzyme often occurs. In addition, the selections of supports are also significant **[1-5]**.

The immobilized enzyme supports must be made suitable for type of enzymes and their application to prevent a leaching out during the reactions and maintain a high level of enzyme activity. Recently, a hierarchical porous carbon monolith synthesized by resorcinol-formaldehyde (RF) gel has been studied **[6]**. The hierarchical porous carbon monoliths containing macropore and micropore are an attractive structure demonstrated as candidates for enzyme immobilization, due to their fairly uniform, adjustable pore sizes and structures, large surface area and high micropore volume. Moreover, it could easily be synthesized and tailor-made for specific applications **[7]**. The carbon monolith is suitable to use as the adsorbent operated under continuous condition, because of the macropore allows fluid flow under low back pressure and high

convective mass transfer **[8]**. Therefore, hierarchical porous carbon monolith has a great potential material to use as the support for enzyme immobilization.

Among of enzymes, lipases are the most attractive and promising enzymes for industrial processes. Lipases are versatile enzyme that able to catalyze for wild reaction in hydrolysis, transesterification, esterification and enantioselective biotransformation at very mild conditions. Thus, the lipases have been used in several applications for food, chemical and pharmaceutical industries. Moreover, lipases are popular used in biodiesel production for transesterification reactions of organic feedstock including fresh or waste vegetable oils, animal fats, and oilseed plants **[9, 10]**.

In this research, the improvements of hierarchical porous carbon monoliths for immobilization of *Candida rugosa* lipase are studied. The hierarchical porous carbon monoliths with different characteristics obtained from carbonization and activation of RF gels are used as the supports. Physical absorption by circulation of enzyme solutions through the column packed carbon monolith is applied for immobilization technique. The optimal conditions for immobilization and the effects of structures of carbon monoliths on immobilized lipase properties are investigated.

1.2 Objective of this research

The hierarchical porous carbon monoliths obtained from carbonization and activation of resorcinol-formaldehyde (RF) gels are used as supports for immobilization of *Candida rugosa* lipase by physical adsorption technique. The immobilizations of enzyme are carried out by circulating enzyme solution using peristaltic pump through the column packed carbon monolith.

The objectives in this work can be separated into three parts as follows:

1. To study on immobilization technique (recirculation of enzyme solution), optimal conditions for the immobilization process and immobilized lipase properties.

2. To study on the effects of oxygen on surface and porous properties of carbon monolith on immobilization of lipase.

3. To study on properties of immobilized enzyme columns.

1.3 Scopes of work

All experiments in this research are performed in laboratory scale. The scopes for study in this work are divided into two main sections as shown in Figure 1.1.

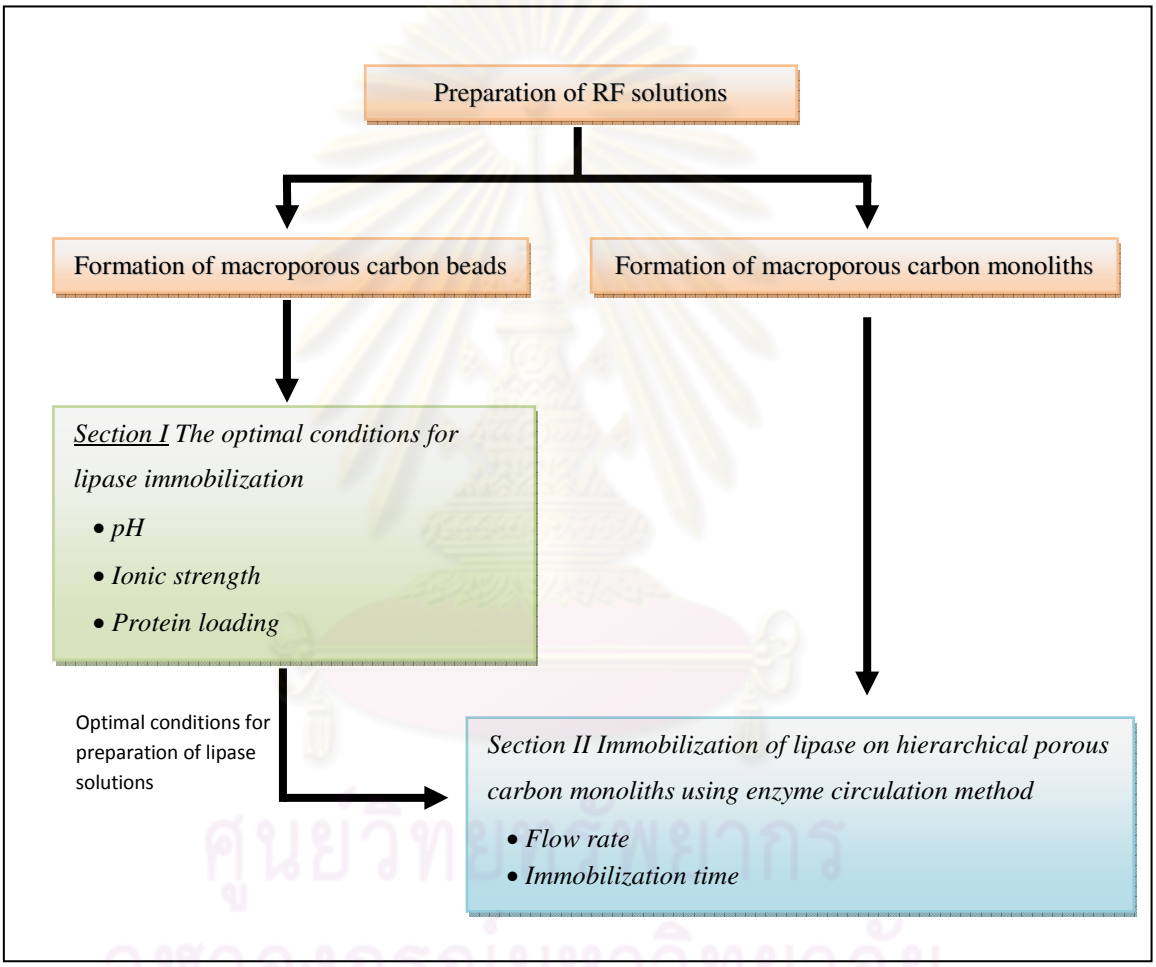

Figure 1.1 Schematic diagrams of the scopes in this work

Section I The optimal conditions for lipase immobilization

In this section, macro/micro porous carbon beads are used as supports to use small amount of enzyme. The carbon beads are conducted by thermal activation of RF gels.

The primary conditions for preparation of lipase are studied as follows:

- The pHs of buffer solutions are studied in the range of 5-9.
- The ionic strengths (or concentration) of buffer solutions are studied in the range of 10-500 mM.
- The protein loadings are studied in the range of 1-8 mg/ml.

Section II Immobilization of lipase on hierarchical porous carbon monoliths using enzyme circulation method

The hierarchical porous carbon monoliths are used as immobilized *Candida rugosa* lipase supports. The optimal conditions used for preparation of enzyme solutions are obtained from Section I. The flow rates of enzyme solution are studied in the range of 10-55 ml/min. The oxygen on surface and porous properties of hierarchical porous carbon monoliths which has an effect on immobilization of lipase as well as the properties of immobilized enzyme columns such as maximum velocity, V_{max} and column kinetics, K are investigated.

ศูนย์วิทยทรัพยากร
จุฬาลงกรณ์มหาวิทยาลัย

CHAPTER II

THEORETICAL BACKGROUND AND LITERATURE REVIEWS

2.1 Hierarchical porous carbon monolith

2.1.1 Resorcinol-formaldehyde gels

Resorcinol–formaldehyde (RF) gels are the porous material classified in family of phenolic resins. The first RF gel was produced by Pekala *et al* **[11]**. Carbon gels were also obtained by carbonization of RF gels in an inert atmosphere. Since, the carbon gels are porous materials that display very interesting features about their structural characteristics because they are very sensitive to the conditions used during gel synthesis and processing **[12]**. Thus, there is a remarkable potential for designing and tailoring these materials to fit specific application. RF and carbon gels have high porosity (>80%) and high surface areas (400–900 m^2/g). Carbon gels are especially expected to be used as adsorbents, electric double-layer capacitors, and materials for chromatographic separation. Furthermore, the carbon RF gels are also used as the supports for the catalyst and enzyme. RF gels are the precursors of carbon gels, and the porous properties of carbon aerogels depend on the porous properties of RF aerogels.

2.1.2 Synthesis of RF gels and carbon gels

Highly cross-linked and transparent inorganic hydrogels can be synthesized by sol–gel polycondensation of metal areas alkoxides. RF hydrogels (organic hydrogels) can also be as prepared by sol–gel polycondensation of resorcinol (R) formaldehyde (F) in a slightly basic aqueous solution. The mechanisms of sol-gel polycondensation reaction of RF gels are shown in Figure 2.1 – 2.2.

Carbon gels can be obtained following different procedures **[1]**, but the preparation mainly consists of three steps: (i) gel synthesis, involving the formation of a three-dimensional polymer in a solvent (gelation), followed by a curing period, (ii) gel

drying, where the solvent is removed to obtain an organic gel, and finally (iii) pyrolysis under an inert atmosphere to form the porous carbon material, i.e. the so-called carbon gel **[12, 13]**.

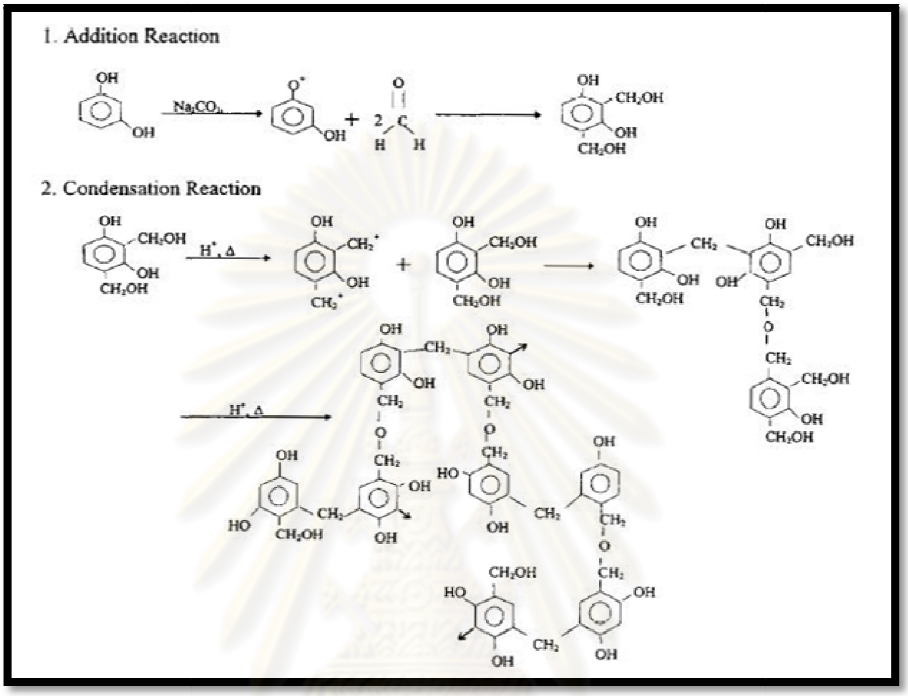

Figure 2.1 Reaction mechanism of the sol-gel polymerization of resorcinol with formaldehyde **[14]**

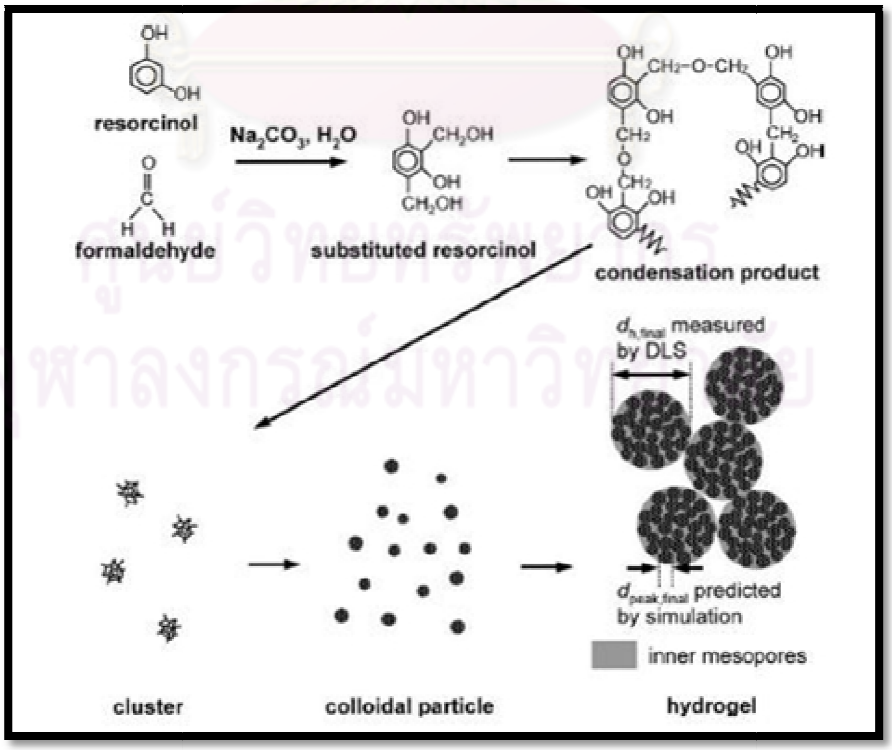

Figure 2.2 Schematic diagram of the sol-gel polycondensation of a RF solution **[15-17]**

Yamamoto *et al.* **[18]** studied the growth rates of colloidal particles formed during the early stage of the sol-gel transition and the time required for the colloidal particles to form a firm network structure could be related to the ratio of catalyst to water (C/W) of the starting RF solution. The results indicated that the molecular weight of colloidal particles increased with the progress of the sol-gel transition, the rate of which was also affected by the value of C/W. The time required for network structure formation also depended on C/W, and decreased with increasing C/W.

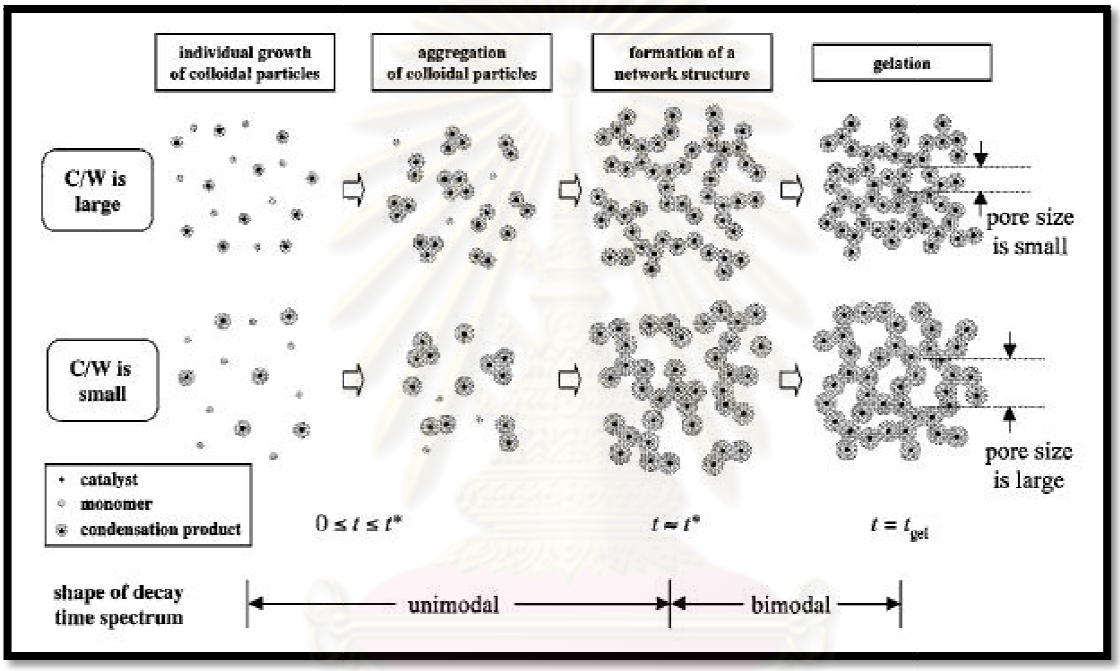

Figure 2.3 Structure formation during the sol-gel transition **[18]**

The effects of drying methods on porosity of carbon gels were also studied by Yamamoto *et al*. The resorcinol–formaldehyde hydrogels were synthesized by sol–gel polycondensation of resorcinol with formaldehyde in a slightly basic aqueous solution. RF cryogels, RF xerogels, and RF xerogels (MW gels) were respectively prepared from RF hydrogels by freeze drying, hot air drying, and microwave drying. Carbon cryogels, carbon xerogels and carbon MW gels were subsequently obtained by pyrolyzing RF drygels in an inert atmosphere. Carbon cryogels showed high mesoporosity over wide ranges of the molar ratio of resorcinol to catalyst (R/C) and the ratio of resorcinol to water (R/W) used in sol–gel polycondensation. Although RF xerogels had a few mesopores, carbon xerogels had no mesopores. Carbon MW gels showed mesoporosity if appropriate values of R/C and R/W were selected **[19]**.

Lin and Ritter studied the effect of initial synthesis pH of the RF solution on the carbon gels **[14]**. Typically, a lower initial pH yielded carbon xerogels with a higher surface area and pore volume, and a broader pore size distribution. Generally, Na_2CO_3 was used as a basic catalyst for preparation of RF solution however the acidic catalyst was also used **[20]**.

A. Siyasukh *et al.* **[6]** synthesized the hierarchical porous carbon monolith using two steps. For the first step, a macroporous interconnected carbon monolith was prepared by ultrasonic irradiation during sol-gel polycondensation. Second step, mesopores were induced in the monolith by $Ca(NO_3)_2$ impregnation followed by CO_2 activation. The results indicated that higher ultrasonic power led to broader macropore size distribution, larger mean pore diameter and larger macropore volume of interconnected carbon monolith while the second step played crucial role on surface properties such as surface area and pore volume. In the second step, mesopore could be successfully generated on macroporous interconnected carbon monolith by $Ca(NO_3)_2$-impregnation and CO_2 activation.

2.1.3 Application of hierarchical porous carbon monolith gels

Since RF gels and carbon gels were easy to synthesized and controlled porosity, they could be made to fit for specific applications. In additions, they were fairly uniform, adjustable pore sizes and structures, large surface area and high micropore volume. Moreover, they were suitable to use in operation under continuous condition, because the macropore allows fluid flow under low back pressure and high convective mass transfer. Therefore, hierarchical porous monolith had a great potential material to use for many applications such as catalyst or enzyme immobilization, HPLC monolithic column, membrane emulsification, electro catalyst support etc. Furthermore, one good example in the application of the hierarchical porous monolith was to use this material for a capillary column which was suitable for sample analysis in a very small amount **[21-24]**.

2.2 Lipase

2.2.1 *Candida rugosa* lipase

Lipases or triacylglycerol lipases are the most widely used as the biocatalysts of the hydrolysis of triacrylglycerides. Moreover, lipase catalyst reactions of water insoluble substrates and the presence of the water/lipid interface is a usual prerequisite for efficient catalysis. This unique property known as interfacial activation may differ for each specific lipase. Lipase from different organisms vary greatly in size, the smallest have molecular masses of 20-25 kDa while the largest are 60-65kDa **[25, 26]**.

The lipases are classified in EC 3.1.1.3 whose each numeral indicate the following groups of enzymes:

E.C.3	Hydrolysis
E.C.3.1	Acting on ester bonds
E.C.3.1.1	Carboxylic ester hydrolases
E.C.3.1.1.3	Triacylglycerol lipase

The success of lipase in industrial applications is due to its specific properties and price, which depends on its source. Lipases are found in most organisms from the animal, plants and microbes **[27]**. Within the hydrolase-based biocatalysis, lipases from *Candida rugosa* were firstly described as early as in the sixties, by isolating the yeast from natural soils due to its powerful lipase production capacity. Later on, two isoenzymes–initially called LipA and LipB were identified, purified and genetically characterized. Nowadays it is well established that at least seven genes are involved in the *C. rugosa* lipase-producing machinery, being five of them (Lip1–Lip5) fully biochemically characterized. The LipA/LipB nomenclature has been practically abandoned, and a new one based on numbers is often used: Lip1- Lip7 **[28, 29]**.

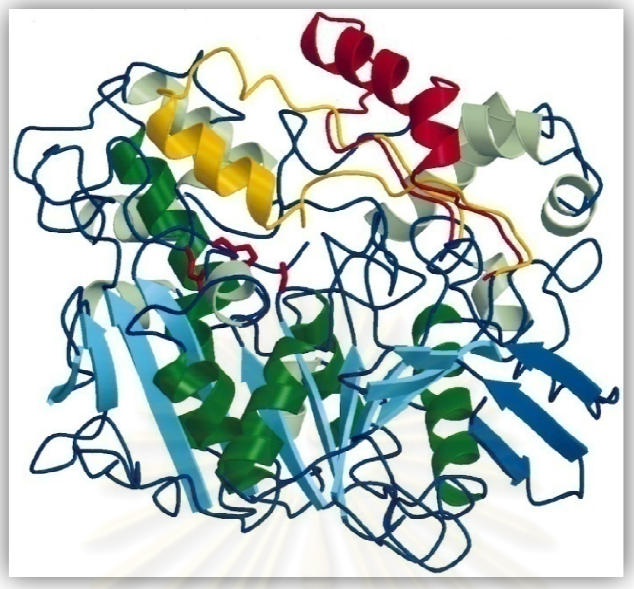

Figure 2.4 Structure of *Candida rugosa* lipase **[28]**

2.2.2 Enzymatic reaction of lipase

Lipase is a powerful tool for catalyzing of the several reactions which not only hydrolysis, but also esterification and transesterification reactions involving water-insoluble esters. In contrast to esterase, lipases are activated only when adsorbed to an oil-water interface and do not hydrolyze dissolved substrates in bulk solution **[26]**.

The main categories into which lipase catalyzed reactions may be classified are as follows:

i. Hydrolysis:

$$R_1COOR_2 + H_2O \longrightarrow R_1COOH + R_2OH$$

ii. Synthesis:

Reactions under this category can be further classified:

a) Esterification

$$R_1COOH + R_2OH \longrightarrow R_1COOR_2 + H_2O$$

ศูนย์วิทยทรัพยากร
จุฬาลงกรณ์มหาวิทยาลัย

b) Interesterification

$R_1COOR_2 + R_3COOR_4 \longrightarrow R_1COOR_4 + R_3COOR_2$

c) Alcoholysis

$R_1COOR_2 + R_3OH \longrightarrow R_1COOR_3 + R_2OH$

d) Acidolysis

$R_1COOR_2 + R_3COOH \longrightarrow R_3COOR_2 + R_1COOH$

The last three reactions are often grouped together into the single term transesterification.

2.2.3 Applications of lipase

Lipases are the most broadly used in oil hydrolysis. In addition to hydrolysis, they catalyze alcoholysis, amidolysis and inter-esterification. Hence lipases have tremendous potentials in several applications such as food technology, pharmaceutical, leather, textile, cosmetic, biodiesel production and chemical industries etc. However, its low stability and activity or selectivity coupled with the high cost prohibits its use in industrial hydrolytic reactions.

2.3 Immobilization of enzyme

There are several reasons for the preparation and use of immobilized enzymes. In addition to a more convenient handling of enzyme preparations, the two main targeted benefits are (1) easy separation of the enzyme from the product, and (2) reuse of the enzyme. Sometimes, the immobilization of enzyme can help to improve the enzyme stability.

Easy separation of the enzyme from the product simplifies enzyme applications and supports a reliable and efficient reaction technology. On the other hand, reuse of enzymes provides cost advantages which are often an essential prerequisite for

establishing an enzyme-catalyzed process in the first place. The properties of immobilized enzyme preparations are governed by the properties of both the enzyme and the carrier material. The specific interaction between the latter provides an immobilized enzyme with distinct chemical, biochemical, mechanical and kinetic properties. The suitable supports and immobilization technique for practical applications should maintain a high level of enzyme activity while preventing a possible leaching out during the reaction **[3, 30]**.

Table 2.1 Selected characteristic parameters of immobilized enzymes **[30]**

Enzyme	*Biochemical properties* molecular mass, prosthetic groups, functional groups on proteinsurface, purity (inactivating/protective function of impurities) *Enzyme kinetic parameters* specific activity, pH-, temperature profiles, kinetic parameters for activity and inhibition, enzyme stability against pH, temperature, solvents, contaminants, impurities
Carrier or support	*Chemical characteristics* chemical basis and composition, functional groups, swelling behavior, accessible volume of matrix and pore size, chemical stability of carrier *Mechanical properties* mean wet particle diameter, single particle compression behavior, flow resistance (for fixed bed application), sedimentation velocity (for fluidized bed), abrasion (for stirred tanks)
Immobilized enzyme	*Immobilization method* bound protein, yield of active enzyme, intrinsic kinetic parameters (properties free of mass transfer effects) *Mass transfer effects* consisting of partitioning (different concentrations of solutes inside and outside the catalyst particles), external and internal (porous) diffusion; this gives the effectiveness in relation to free enzyme *determined under appropriate reaction conditions,* *Stability* operational stability (expressed as activity decay under working conditions), storage stability

ศูนย์วิทยทรัพยากร
จุฬาลงกรณ์มหาวิทยาลัย

Immobilized enzyme	*"Performance"*
(next)	productivity (amount of formed product per unit or mass of enzyme)
	enzyme consumption (e.g. units kg–1 product, until half-life)

2.3.1 Immobilization methods

There are several methods for immobilization of enzymes having been reported in the literatures review such as adsorption, covalent linking, entrapping and encapsulation. The immobilization methods are classified as shown in Figure 2.5. However, adsorption and covalent bonding are popular techniques for the preparation of immobilize enzyme. They have shown several advantages over enzymes in bulk solution.

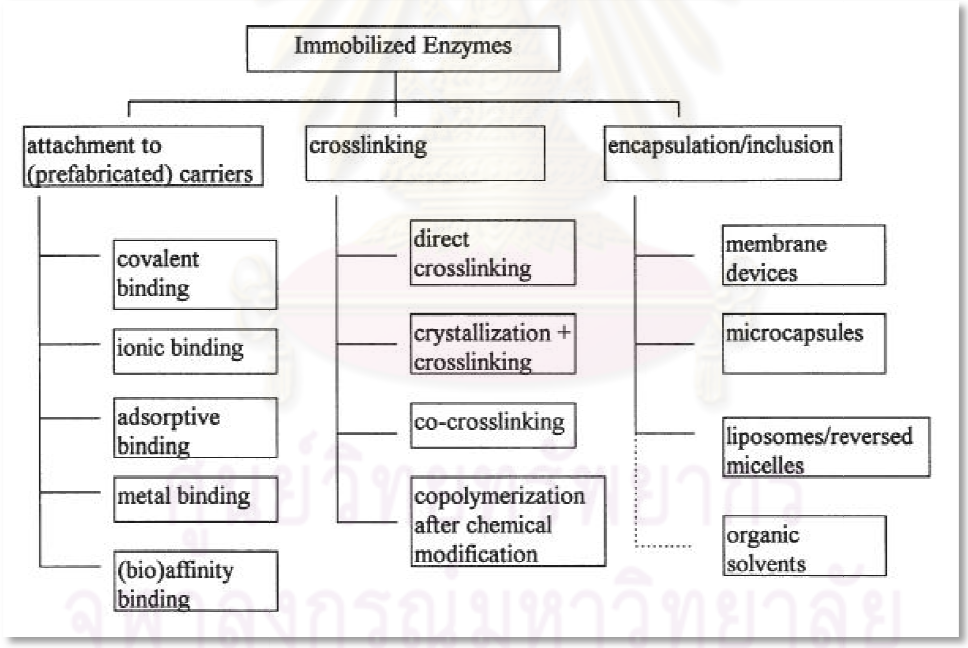

Figure 2.5 Classification of immobilization methods **[30]**

The immobilization methods are discussed briefly as following:

Physical adsorption is the simplest method and involves reversible surface interactions between enzyme and the support material. The forces involved are mostly electrostatic, such as Van der Waals interactions, hydrophobic interactions, hydrogen

bonds, ionic bonds, although hydrophobic bonding can be significant. These forces are very weak, but sufficiently large in number to enable reasonable binding.

Covalent linkage involves the formation of a covalent bond between the enzyme and support material. The bond is normally formed between functional groups present on the surface of the support and functional groups belonging to amino acid residues on the surface of the enzyme.

Entrapment differs from adsorption and covalent binding in that enzyme molecules are free in solution, but restricted in movement by the lattice structure of a gel. Entrapment can be achieved by mixing an enzyme with a polyionic polymer material and then cross linking the polymer with multivalent cations in an ion-exchange reaction to from a lattice structure that traps the enzyme. Alternatively, it is possible to mix the enzyme with chemical monomers that are then polymerized to from a cross linked polymeric network, trapping the enzyme in the interstitial spaces of the lattice.

Encapsulation can be achieved by enveloping the biological components within various forms of semi permeable membranes. It is similar to entrapment in that the enzymes and cell are free in solution, but restricted in space. Large proteins or enzymes cannot pass out of or into the capsule, but small substrates and products can pass freely across the semi-permeable membrane.

The comparison of different advantages and disadvantages of each immobilization methods depending upon its natures and applications are shown in Table 2.2.

Table 2.2 Comparison of each enzyme immobilization techniques

Characteristics	Adsorption	Covalent binding	Entrapment	Encapsulation
Preparation	Simple	Difficult	Difficult	Simple
Cost	Low	High	Moderate	High
Binding force	Variable	Strong	Weak	Strong
Enzyme leakage	Yes	No	Yes	No
Applicability	Wide	Selective	Wide	Vary wide

Table 2.2 (next) Comparison of each enzyme immobilization techniques

Characteristics	Adsorption	Covalent binding	Entrapment	Encapsulation
Running problems	High	Low	High	High
Matrix affects	Yes	Yes	Yes	No
Large diffusional barriers	No	No	Yes	Yes
Microbial protection	No	No	Yes	Yes

2.3.2 Review papers for Immobilization of enzyme

Immobilized lipases are considered hereafter as lipases which are localized in a defined region of space, which is enclosed by an imaginary or material barrier which allows for physical separation of the enzyme from the bulk reaction medium, and which is at the same time permeable to reactant and product molecules.

There are several literatures which have been used in studies of immobilized lipases as following.

T. Chaijitrsakool *et al*. **[31]** studied on immobilization of *Bacillus licheniformis* serine protease in resorcinol-formaldehyde carbon gels (RFCs) of different pore characters. This paper demonstrated that the first time for the use of RFCs as enzyme carriers. RFCs derived with (RF1) and without (RF2) cationic surfactant (trimethylstearylammonium chloride; C18) resulted in predominantly microporous, and mesoporous characters, respectively. It was found that support pore size and volume were key parameters in determining immobilized enzyme loading, specific activity, and stability. In addition, RF2 was found to be a better support in terms of serine protease operation and storage stability. Suitable mesopore size likely helped preventing immobilized enzyme from structural denaturation due to external forces and heat. However, immobilized enzyme in RF1 gave higher specific activity than in RF2 and soluble enzyme. Enzyme leaching was found to be problematic in both supports, nonetheless, higher desorption was observed in RF2.

N. Dizge *et al*. **[7]** carried out lipase-catalyzed synthesis of fatty acid methyl esters (biodiesel) from various vegetable oils using lipase immobilized onto a novel microporous polymeric matrix (MPPM) as a low-cost biocatalyst. Three aspects of the process: (a) MPPM synthesis (monolithic, bead, and powder forms), (b) microporous polymeric biocatalyst (MPPB) preparation by immobilization of lipase onto MPPM, and (c) biodiesel production by MPPB were studied. *Thermomyces lanuginosus* lipase was covalen tly attached onto MPPM by enzyme recirculation method with 80%, 85%, and 89% immobilization efficiencies using bead, powder, and monolithic forms, respectively. It could be seen that MPPB in monolithic form show the highest immobilization efficiencies than the others. Immobilized enzymes were successfully used for the production of biodiesel using sunflower, soybean, and waste cooking oils. It was shown that immobilized enzymes retain their activities during 10 repeated batch reactions at 25 ^{o}C, each lasting 24 h.

M. Shakeri *et al*. **[32]** studied on immobilization of *Rhizopus oryzae* lipase (ROL) onto SBA-15 (a pure silica) and PMO (an organosilica with ethane bridging groups) with different structural chemical compositions, but with relatively similar physical characteristics. The adsorption capacity of PMO for ROL immobilization was higher than that of SBA-15 as a result of the stronger combination of electrostatic and hydrophobic interactions between ROL and PMO compared to the electrostatic interaction between ROL and SBA-15. ROL immobilized onto PMO showed a higher trans-esterification reaction activity than that immobilized onto SBA-15 and that of free ROL.

ศูนย์วิทยทรัพยากร
จุฬาลงกรณ์มหาวิทยาลัย

CHAPTER III

EXPERIMENTAL PROCEDURE

All experiments in this research are carried out in laboratory-scale to study the immobilization of *Candida rugosa* lipase on hierarchical porous carbon monolith by physical absorption technique. The carbon monoliths with various porous characteristics synthesized by sol-gel polycondensation of resorcinol with formaldehyde are used as supports. In addition, the optimization conditions for lipase immobilization are studied. The enzymatic activities of immobilized lipase and the effects of structure of carbon monolith on lipase immobilization are investigated.

The chemicals, equipments, characterizations and experimental methods in this research are described in this chapter.

3.1 Chemical reagents

The chemical reagents used in this research are showed in Table 3.1.

Table 3.1 List of chemical reagents in this research

Chemical reagents	**Grade**	**Manufacturer**
1. Resorcinol ($C_6H_4(OH)_2$)	99.8% BDH/38	Fluka, German
2. Formaldehyde (HCOH)	analytical grade	Ajax Finechem, New Zealand
3. Nitric acid (HNO_3)	analytical grade	Ajax, New Zealand
4. Dionized water	-	Production from MilliQ apparatus (Millipore, Bedford, MA).
5. Calcium nitrate tetrahydrate ($Ca(NO_3)_2 \cdot 4H_2O$)	analytical grade	Ajax Finechem, New Zealand
6. Nitrogen (N_2)	purity 99.999%	Thai Industrial Gas (TIG), Thailand
7. Carbon dioxide (CO_2)	purity 99.8%	Thai Industrial Gas (TIG), Thailand

Table 3.1 (next) List of chemical agents in this research

Chemical agents	Grade	Manufacturer
8. *Candida rugosa* lipase type VII	analytical grade	Sigma, U.S.A.
9. *p*-Nitrophenyl palmitrate (*p*-NPP)	analytical grade	Sigma, U.S.A.
10. Bovine serum albumin, BSA	analytical grade	Merck, Germany
11. Bradford's reagent	analytical grade	Biorad, U.S.A
12. n-Butanol	analytical grade	Carlo erba, Italy
13. *t*-butanol	analytical grade	Carlo erba, Italy
14. Ethanol	analytical grade	Lab scan, Thailand
15. Di-potassium hydrogen phosphate (K_2HPO_4)	analytical grade	Scharlau, Spain
16. Potassium di-hydrogen phosphate (KH_2PO_4)	analytical grade	Merck, Germany
17. Tris (hydroxymethyl) aminomethane hydrochloride ($C_4H_{11}NO_3ClH$)	analytical grade	Scharlau, Spain

3.2 Equipments

3.2.1 Basic equipments

- Desiccator
- Digital Balance
- Filter paper, Whatman No.1
- Horizontal furnace
- Magnetic bar
- Magnetic stirrer
- Microplate spectrometer
- Micropipette
- Microrefrigerated centrifuge: model 5417
- pH meter
- UV-VIS spectrophotometer
- Vacuum pump
- Vortex
- Water bath

ศูนย์วิทยทรัพยากร
จุฬาลงกรณ์มหาวิทยาลัย

3.2.2 Column reactor apparatus

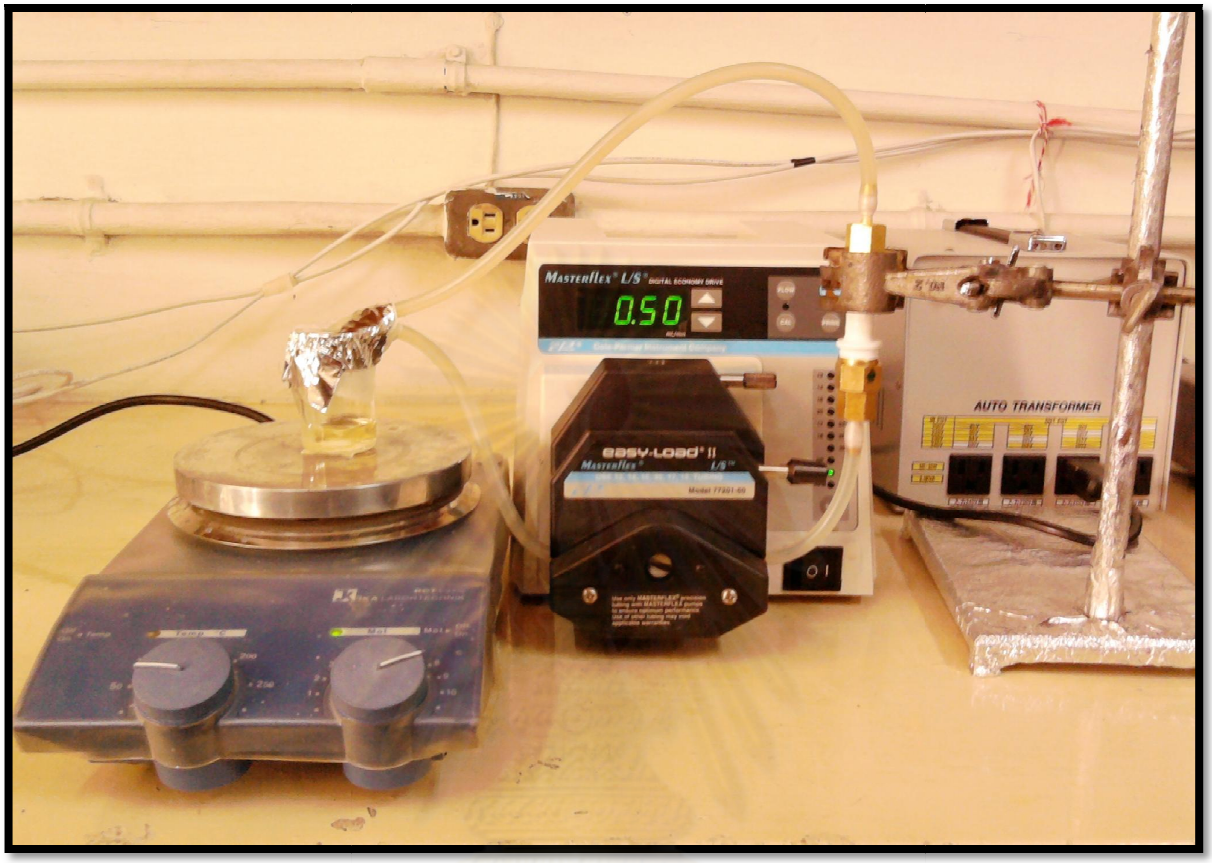

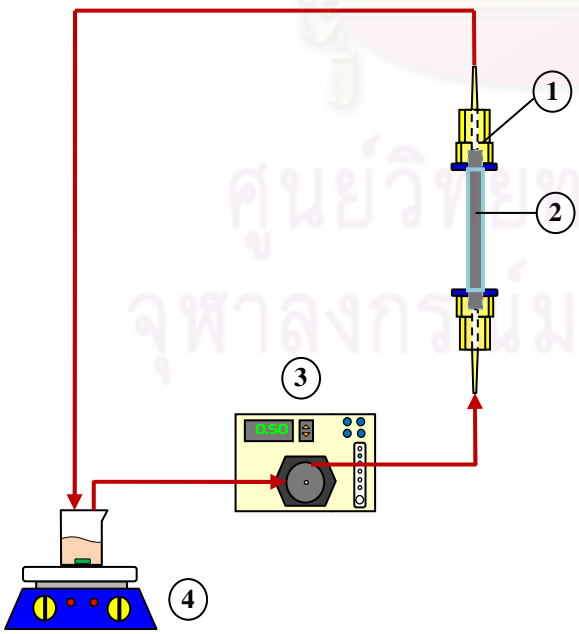

Figure 3.1 : Illustration of column reactor set up for step of enzyme immobilization and activity assays, (1) column holder, (2) glass column, (3) digital peristaltic pump and (4) magnetic stirrer.

The immobilization process and activity assay are preformed with column reactor apparatus as showed in Figure 3.1 which contain in four parts as followed.

- Part (1) is the brass column holder.
- Part (2) is the glass column for the carbon monolith packing having inside diameter and length are 10 mm and 6 cm, respectively. (see 3.4.3.1)
- Part (3) is the digital peristaltic pump.
- Part (4) is the magnetic stirrer.

3.3 Characterizations

1. Porosity is characterized by nitrogen adsorption – desorption at – 196 ^{o}C (BEL; BELSORP – mini).

1.1. BET surface (S_{BET}) is determined by BET equation.

1.2. micropore volume (V_{mic}) is calculated by t – method.

2. Microstructure was characterized by SEM (Scanning Electron Microscope) (JEOL; JSM – 5800LV).

3. Interconnected macropores size distribution and volume are measured by mercury intrusion technique by Micromeritics, Pore-Sizer-9320.

4. Fourier Transform Infrared (FTIR) spectra were recorded using spectrometer (Perkin Elmer, 1615).

5. A decrease in weight of the obtained carbon monoliths, % burn-off, was measured after carbonization and activation.

6. Protein content of lipase was determined by Bradford method using UV-VIS spectrophotometer (Thermo scientific, UK).

7. Enzyme activity was established by absorbance at 410 nm using UV-VIS spectrophotometer (Thermo scientific, UK).

3.4 Experimental procedures

The experimental procedures in this research can be divided into two main sections. First, the optimization conditions for lipase immobilization on macroporous carbon beads are studied. Second is immobilization of lipase on hierarchical porous carbon monoliths using enzyme circulation method. Both macroporous carbon beads and hierarchical porous carbon monoliths are obtained from resorcinol-formaldehyde (RF) gels.

3.4.1 Preparation of the carbon bead and monolith supports

The preparation process of macroporous carbon beads and hierarchical porous carbon monolith are shown in Figure 3.2.

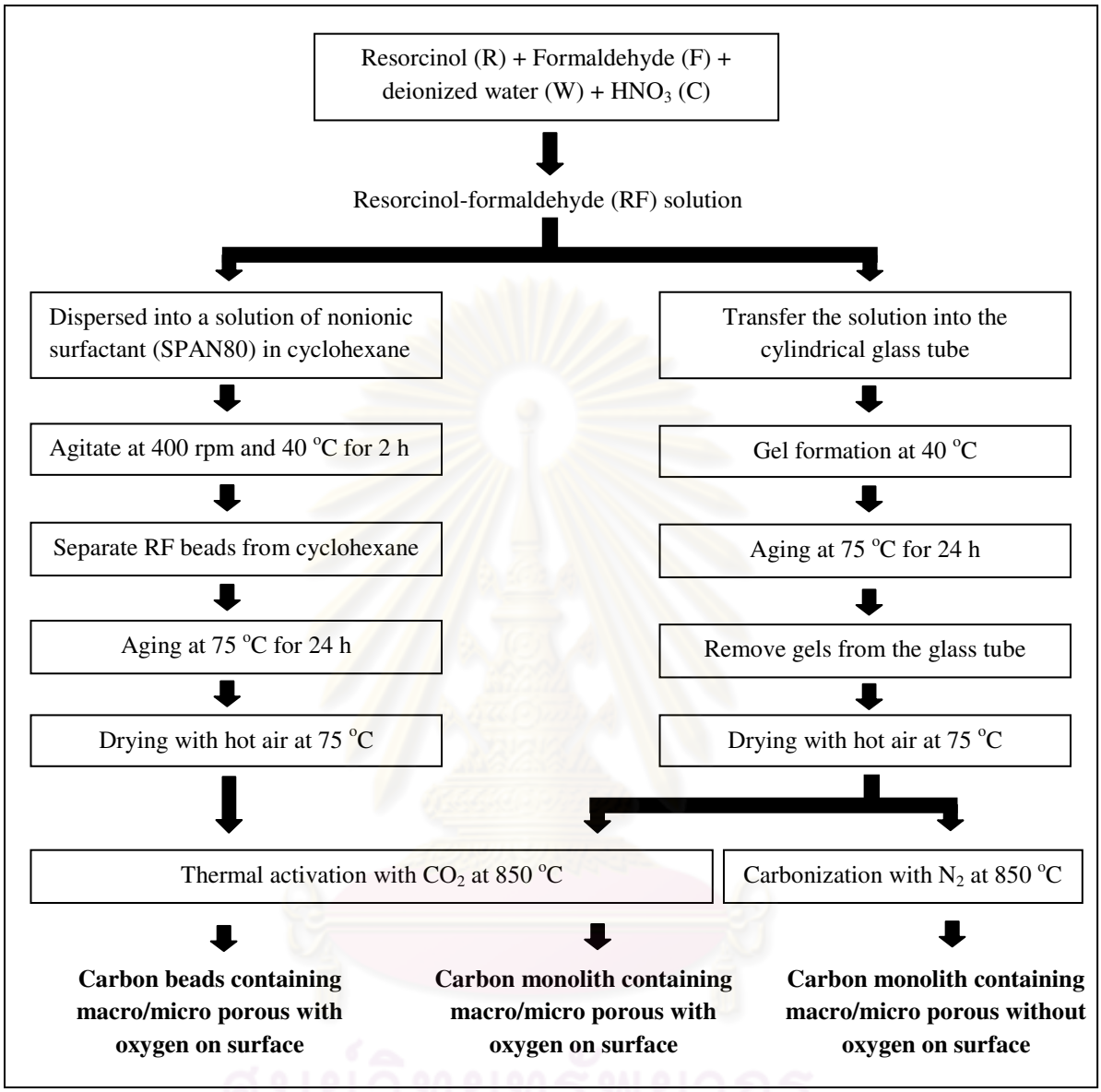

Figure 3.2 Preparation of carbon beads and carbon monolith diagrams

ศูนย์วิทยทรัพยากร
จุฬาลงกรณ์มหาวิทยาลัย

3.4.1.1 Preparation of RF solutions

Resorcinol-formaldehyde (RF) solutions were prepared from resorcinol with formaldehyde in de-ionized water. Nitric acid solution 0.5 M is used as a catalyst **[5]**.

Firstly, resorcinol was dissolved into the deionized water and stirring it with magnetic stirrer until complete dissolution. Then, the resorcinol solution was added with formaldehyde solution and followed by adding the solution of 0.5 M of nitric acid. All

solutions were then placed in a temperature controlled bath and RF solutions were obtained.

The molar ratios of resorcinol to formaldehyde (R/F), and resorcinol to water (R/W), and the mole to volume ratio of catalyst to water (C/W) were fixed at 0.5 mol/mol, 0.15 mol/mol, and 0.20 mol/ml, respectively.

3.4.1.2 Formation of macroporous carbon beads

The macroporous carbon beads were used for study the primary immobilization conditions. They were synthesized by RF solutions. Before RF solutions lost their fluidity, they were dispersed into a solution of nonionic surfactant (SPAN80) in cyclohexane. After that, the mixtures were agitated at 400 rpm and 40 ^{o}C for 2 h. RF beads were then separated from cyclohexane, aging at 75 ^{o}C for another 24 h and drying at this temperature until the weight was constant.

Finally macroporous carbon beads were obtained by carbonization of RF beads. The RF beads were conducted by thermal activation under a 50 cm^3-STP flow of CO_2. Samples were heated up to 850 ^{o}C with 10 ^{o}C/min heating rate and kept at this temperature for 30 minutes.

3.4.1.3 Formation of macroporous carbon monoliths containing various pore characteristics

RF solutions were transferred into the cylindrical glass tube where RF gel was formed. After that the gel was sealed at the ends of the tube, followed by 24 h for aging in the oven at temperature of 75 ºC. After aging, the gel was removed from the tube and followed by drying with hot air at 75 ºC until the weight was constant. The dried RF carbon precursors in a monolithic form were obtained. The carbon monolith containing different porous structures was obtained from carbonization in two different methods.

The RF dried-monolith was carbonized in two different methods as follows:

Method I Carbonization with N_2

RF dried-monolith gels were carbonized with N_2 in a quartz tube reactor at 850 ºC for 30 min with 10 ^{o}C/min heating rate. RF carbon monoliths containing macro/micro porous structure were obtained.

Method II Direct thermal activation with CO_2

RF dried-monolith gels were conducted by thermal activation with CO_2 in a quartz tube reactor at 850 ºC for 30 min with 10 ^{o}C/min heating rate. RF carbon monoliths containing macro/micro porous structure and having oxygen on surface were finally obtained after the process.

The carbonization and activation processes in this research are carried out with horizontal furnace reactor as shown in Figure 3.3.

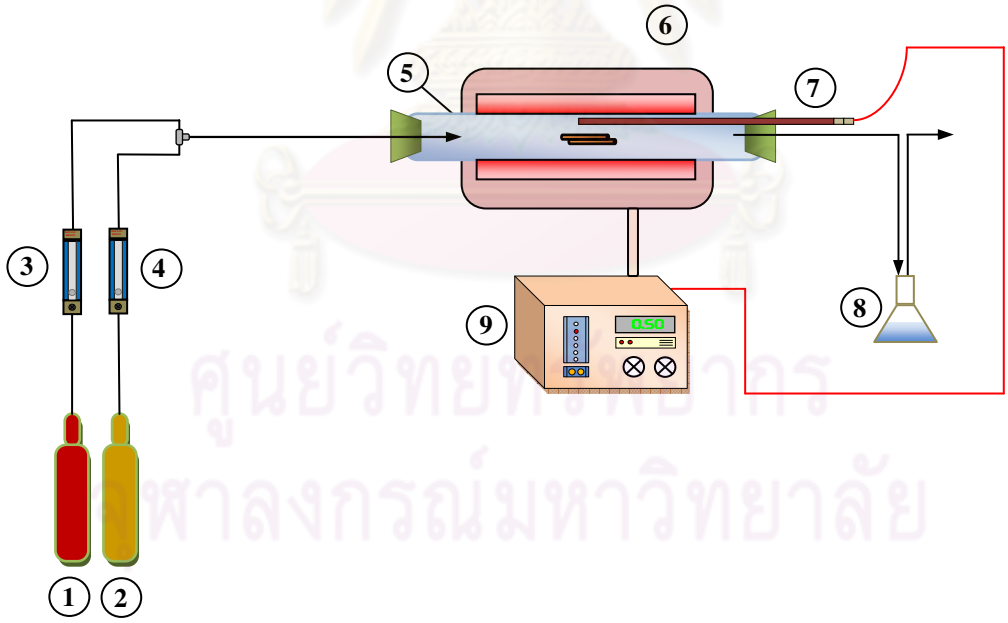

Figure 3.3 : Diagram of the furnace system used in this work, it is composed with (1) N_2 gas container, (2) CO_2 gas container, (3) CO_2 gas flow meter, (4) N_2 gas flow meter, (5) cylindrical quartz tube, (6) furnace, (7) Thermocouple, (8) flask containing alcohol for residual trap and (9) furnace controller box.

3.4.2 The optimization conditions for lipase immobilization

In this section, the important conditions for preparation of enzyme solution before immobilization are studied. Macroporous carbon beads are used in this section in order to decrease the amount of enzymes and their cost. The factors were studied as follows: pH, ionic strength and protein loading.

3.4.2.1 Preparation of lipase immobilization on macroporous carbon beads

In the preparation for immobilization, 0.1 g of carbon bead supports were pre-wet with 3 ml *t*-butanol overnight to exclude the air within the carbon beads. Then, they were filtered and ready for enzyme immobilization.

Upon immobilization, the prepared carbon beads were brought into contact with 3 ml lipase solution in a sealed vessel. The vessel was then placed in an orbital shaker at room temperature for 6 h. Next, the enzyme-loaded carbon beads were washed for five times with phosphate buffer solution. The supernatant and washing solutions were assayed for unbound protein. Finally, they were then filtered, dried in desiccator, and stored at 4 ^{o}C before further used.

3.4.2.2 Enzyme activity assay for immobilized carbon beads

Activity of the free and immobilized lipase was assayed by using 0.5 % (w/v) *ρ*-nitrophenyl palmitate (*p*-NPP) in ethanol as substrate. The reaction mixture consisting of 0.25 ml, 50 mM Tris-HCl buffer, pH 8 containing immobilized lipase or 25 µl of free lipase was initiated by adding 0.25 ml of substrate and mixed for 5 min at room temperature. The reaction was terminated by adding 0.5 ml of 0.25 M Na_2CO_3 followed by centrifugation at 14,000 rpm at 4 ^{o}C for 5 min. The increase of the absorbance at 410 nm produced by the release of *p*-nitrophenol in the enzymatic hydrolysis of *p*-NPP was then measured.

One international unit (IU) of lipase was defined as the amount of enzyme needed to liberate 1µmol of *p*-nitrophenol per minute using *p*-nitrophenyl palmitate as a substrate. Calculation for the unit of enzyme activity was described in Appendix C.

3.4.2.3 Protein assay

The amount of protein content before and after immobilization was determined by Bradford protein assay method. The reaction mixture consisted of 5 µl of sample containing 300 µl of Bradford reagent in 96 well plates and was incubated at room temperature for 5 min, and later measured for the absorbance at 595 nm. Standard curve was prepared to determine concentration of protein using bovine serum albumin (BSA) at the concentration of 0.1-0.6 mg/ml. The amount of protein bound to the enzyme carriers was determined as the difference between the initial and residual protein concentrations in the supernatants. The calculation method was shown in Appendix D.

3.4.3 Immobilization of lipase on hierarchical porous carbon monoliths using enzyme circulation method

This section, the carbon monoliths with hierarchical porous structure are used as immobilized *Candida rugosa* lipase supports. Physical absorption by continuous flowing enzyme solution through the column is applied for immobilization technique. Immobilization conditions (such as flow rate of enzyme and immobilization times) and the effects of characteristics of carbon monolith are investigated.

3.4.3.1 Packing of carbon monolith in the column

The carbon monolith (8 mm in diameter and 6 cm in length) was clad by heat-shrinkable tubing. The encapsulated carbon monolith was then glued into a precut glass tube with epoxy glue. The configuration of the column cross section was illustrated in Figure 3.4. The carbon monolith packed in the column was then ready to be used.

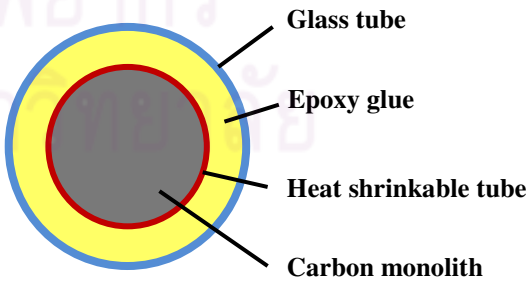

Figure 3.4 Cross section of the column

3.4.3.2 Immobilization of lipase on a column containing hierarchical porous carbon monolith

The column was first wash with 20 ml of *t*-butanol to remove impurities and adjust the surface of carbon monolith for ready to enzyme immobilization.

The immobilization of enzyme was carried out by circulating enzyme solution in the optimization conditions (obtained from section I) by peristaltic pump through the column packed carbon monolith at various enzyme flow rates and immobilization times. The immobilized enzyme column was then washed with 20 ml phosphate buffer solution by circulating for 15 minutes at 55 ml/min flow rate for three times to remove unbound enzyme. The supernatant and washing solutions were assayed for unbound protein. Finally, the immobilized enzyme column was dried in desiccator and stored at 4 ^{o}C.

3.4.3.3 Enzyme activity assays for immobilized carbon monolith

Immobilized lipase activity assays were performed by using transesterification reaction of *p*-nitrophenyl palmitate (*p*-NPP) and butanol resulting in *p*-nitrophenol (*p*-NP). The amount of *p*-nitrophenol was determined by increasing of the absorbance at 410 nm **[7]**.

The solution of *p*-NPP (19 mM) was prepared in *t*-butanol. The reaction mixture comprised of *p*-NPP solution (19 ml) and butanol (1 ml). The reaction mixture was recirculated at the room temperature using a peristaltic pump with a rate of 55 ml/min. The reaction mixtures were taken with interval for 3 h. Then, the sampling of 5 µl was added to 300 µl of triethylamin-ethanol solution (3 µl triethylamine per ml ethanol) in 96 well plates. *p*-NP formed by the enzymatic transesterification reaction was determined at 410 nm. Each of the assays was performed in duplicate and mean values were presented.

CHAPTER IV

RESULTS AND DISCUSSIONS

The results of the experimental are shown in this chapter. Characterizations of the carbon support used in immobilization process, the optimal condition (pH, ionic strength and protein loading) and the effects of two different pore structures of carbon on immobilization of lipase are explained.

4.1 Characterizations of carbon supports

Both of the carbon bead and monolith supports were synthesized from resorcinol-formaldehyde (RF) gels conducted by carbonization with N_2 and the thermal activation with CO_2. The macroporous carbon beads were obtained by carbonization of RF beads conducted by thermal activation under flow of CO_2. The carbon monoliths with (C-CO_2) and without (C-N_2) oxygen on surface were obtained from thermal activation and carbonization, respectively.

4.1.1 Characterization of macroporous carbon beads

The carbon beads were used for study the optimal condition in order to preparation of enzyme solution.

4.1.1.1 Structure of carbon beads

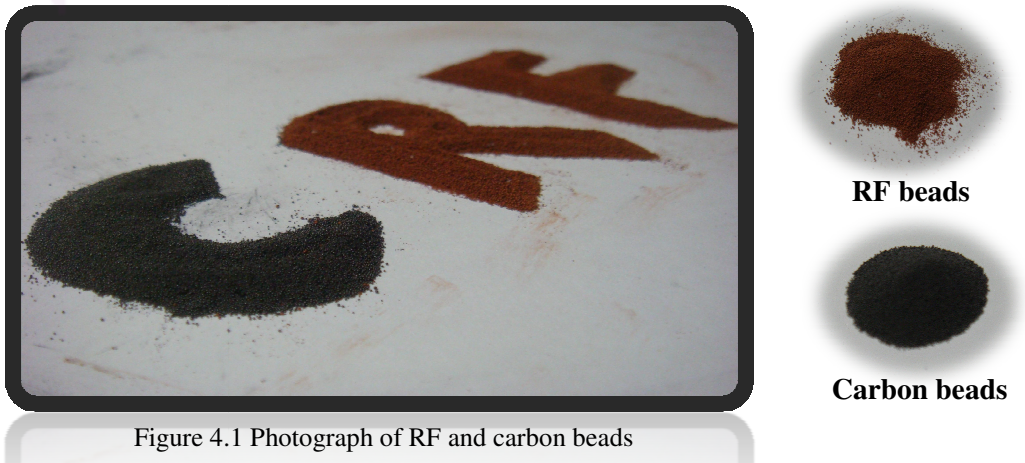

Figure 4.1 Photograph of RF and carbon beads

According to the Figure 4.1, the photograph of the RF beads (before thermal activation) and carbon beads (after thermal activation) are shown.

The SEM images in Figure 4.2 show macro porous structure of carbon beads.

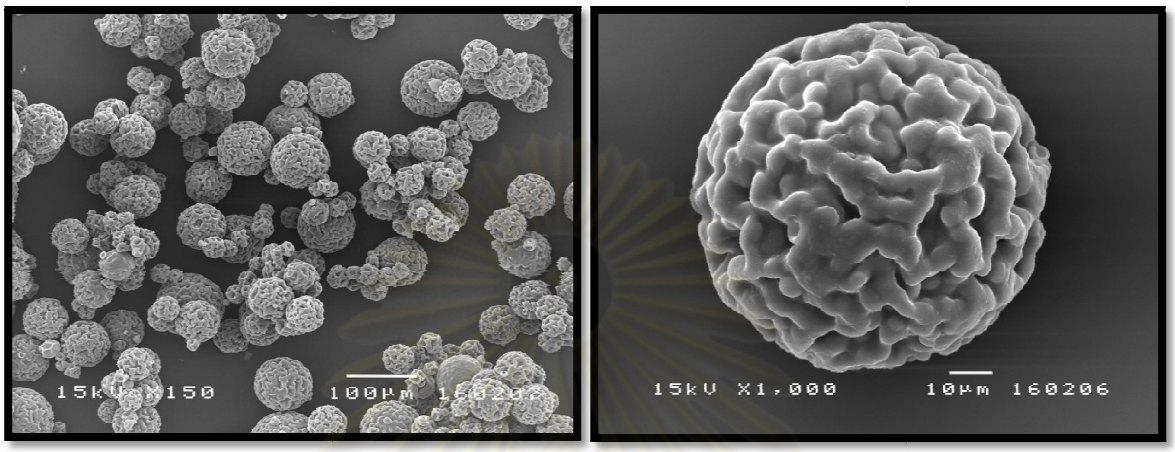

Figure 4.2 SEM micrographs of carbon beads

After thermal activation of RF beads, the sizes of obtained carbon beads are decreased. The particle size distribution of carbon bead is approximately 100µm with narrow distribution as shown in Figure 4.3. The % burn-off of the activated carbon bead is 53.01%.

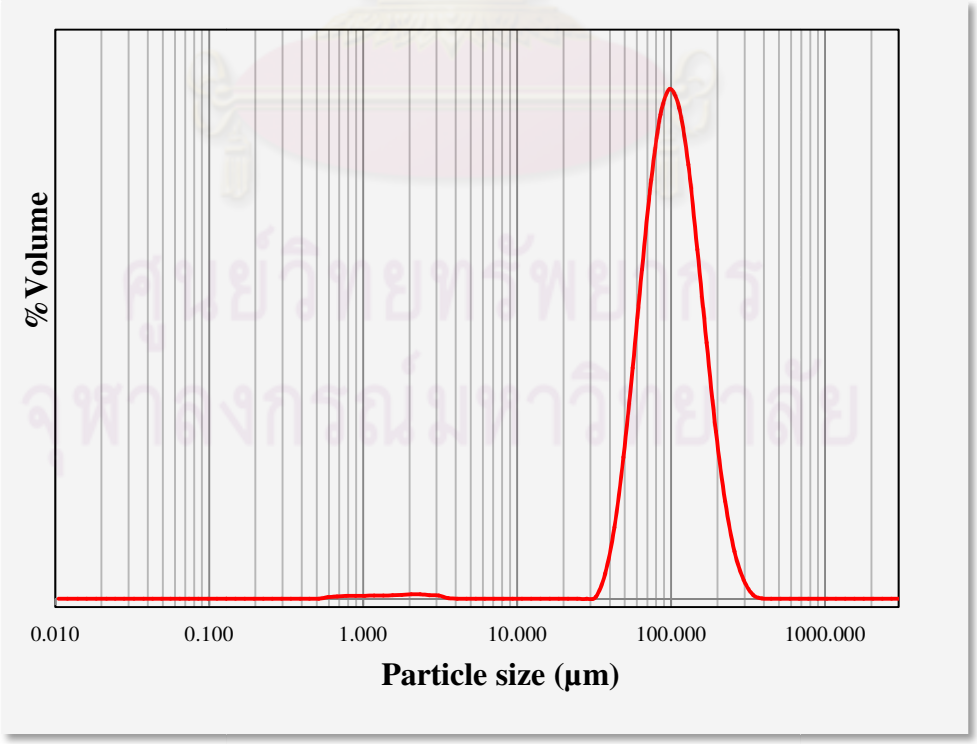

Figure 4.3 Particle size distribution of carbon bead

4.1.1.2 Porous properties of RF and carbon beads

Figure 4.4 shows the adsorption-desorption isotherm of N_2 at 77 K on the carbon bead. For the carbon bead, the isotherms are indicated that IUPAC type I microporous material.

The porosities of the carbon bead determined from the isotherm, the BET specific surface area (S_{BET}) and the micropore volume (V_{mic}) of the carbon beads are 491.12 m^2/g and 0.31 cm^3/g, respectively.

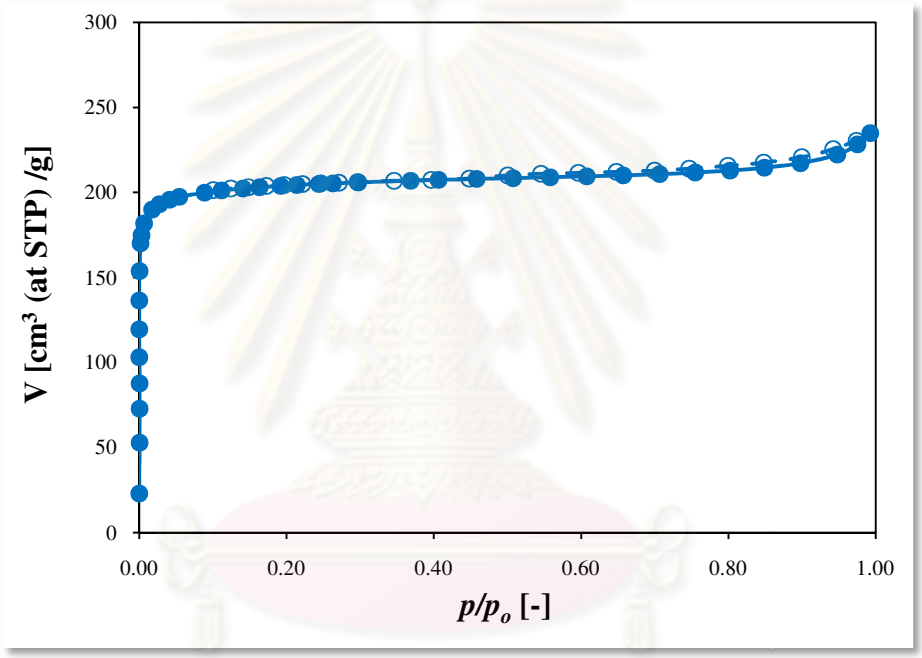

Figure 4.4 N_2 adsorption-desorption isotherm of macroporous carbon bead

4.1.2 Characterization of carbon monoliths

The carbon monoliths were synthesized by two different carbonization methods. First, the carbonization with N_2 was used for preparation of carbon monolith without oxygen on the surface (C-N_2). The second is thermal activation with CO_2 used for generate oxygen on surface of carbon monolith (C-CO_2) **[6]**.

4.1.2.1 Structure of RF and carbon monoliths

The influences of carbonization with N_2 and thermal activation with CO_2 of

the carbon monolith are studied on samples C-N_2 and C-CO_2, respectively.

Table 4.1 Physical properties of RF and carbon monoliths

Sample	Carbonization method	Diameter (mm)	%Reducing volume after carbonization process	%Burn off
RF monolith	-	8.75	-	-
C-N_2	carbonization with N_2	6.96	48.34	56.71
C-CO_2	thermal activation with CO_2	7.06	47.36	64.12

The photograph of RF monolith gels (a), carbon monolith obtained from carbonization with N_2, C-N_2 (b) and thermal activation with CO_2, C-CO_2 (c) are shown in Figure 4.5 which reveal that samples C-N_2 and C-CO_2 are retained in the monolithic structures after carbonization process. The shapes of the C-N_2 and C-CO_2 are similar.

Figure 4.5 Photograph of RF and carbon monoliths

According to Table 4.1, the %Burn off of samples C-N_2 and C-CO_2 are 56.71% and 64.12 %, respectively. The reducing volume of C-N_2 (48.34 %) and C-CO_2 (47.36 %) are slightly different.

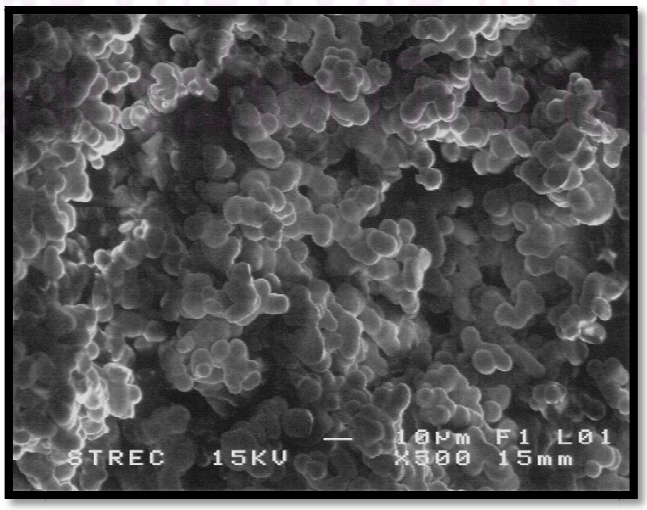

Figure 4.6 The SEM images show the cross-section of RF monolith gels

Macroporous texture of RF and carbon monoliths are observed by SEM images in Figures 4.6 and 4.7. These SEM images confirm the maintenance of interconnected macroporous structure of the C-N_2 and C-CO_2

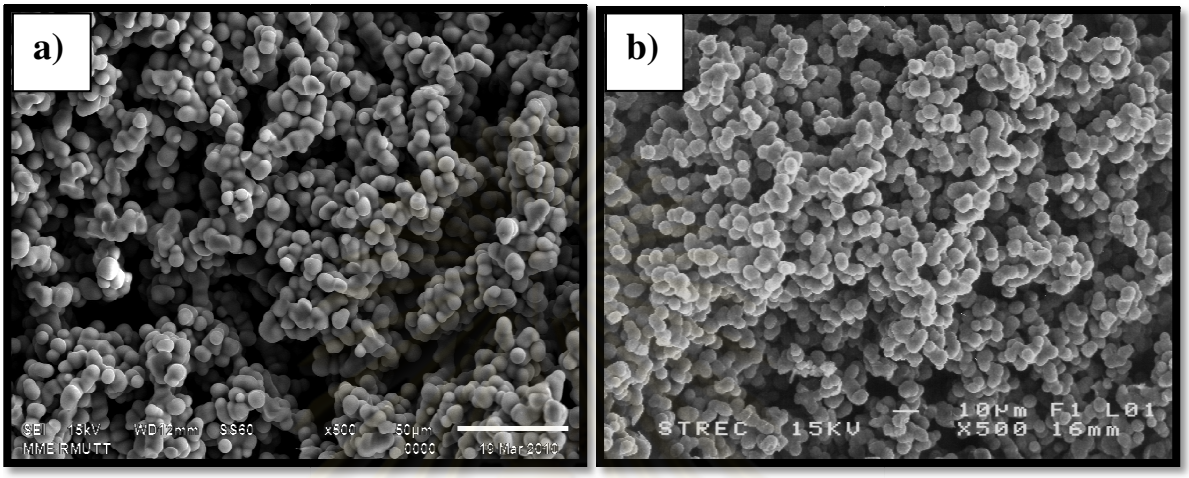

Figure 4.7 The SEM images show the cross-section of carbon monoliths obtain from carbonization, C-N_2 (a) and thermal activation, C- CO_2 (b)

4.1.2.2 Porous properties of RF and carbon monoliths

The macropore diameter of C-N_2 and C-CO_2 are 18.57 µm and 13.49 µm, respectively as shown in Figure 4.8. Moreover, the macropore volume of sample C-CO_2 (0.63 cm^3/g) is slightly smaller than sample C-N_2 (0.65 cm^3/g). It can be seen that the structure of carbon monolith obtained from carbonization with N_2 (C-N_2) shows lower shrinkage than the carbon monolith obtained from thermal activation with CO_2 (C-CO_2) which result in the larger macropore diameter of C-N_2.

Table 4.2 Porosity of carbon monoliths

Samples	Macro pore diameter (µm)	Macropore volume (cm^3/g)	Type of N_2 adsorption-desorption isotherm	Micro pore volume [cm^3/g]	S_{BET} (m^2/g)
C-N_2	18.57	0.65	Type I	0.19	288.73
C-CO_2	13.49	0.63	Type I	0.25	384.95

The N_2 adsorption-desorption isotherms of sample C-N_2 and C-CO_2 are also classified by IUPAC type I microporous material as shown in Figure 4.9. The porous properties of these samples are shown in Table 4.2. From Table 4.2, sample C-N_2 with S_{BET} of 288.73 m^2/g and V_{mic} of 0.19 cm^3/g is synthesized by carbonization with N_2. Sample C-CO_2 prepared from thermal activation with CO_2 has a larger S_{BET} and V_{mic} when compared with sample C-N_2. The S_{BET} and V_{mic} of C-CO_2 are 384.95 m^2/g and 0.25 cm^3/g, respectively.

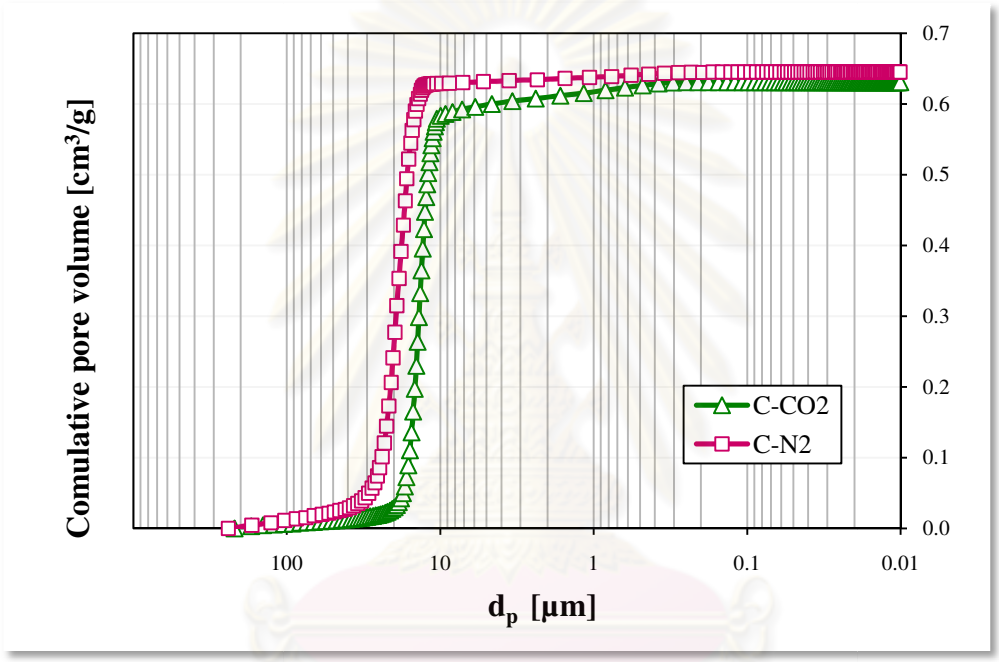

Figure 4.8 Macropore size distributions of C-N_2 and C-CO_2

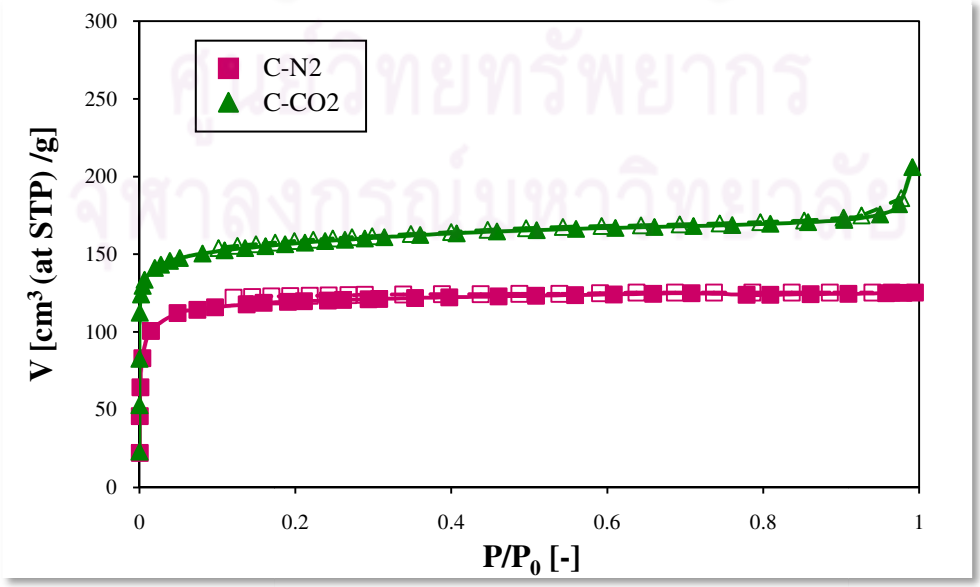

Figure 4.9 N_2 adsorption-desorption isotherms of samples C-N_2 and C-CO_2

4.1.2.3 Oxygenated functional groups on surface of RF and carbon monoliths

From the previous study, the oxygen on surface can be generated by thermal activation which is characterized by FT-IR spectrum. Oxygen on surface of carbon can be found in several form of surface function group binding at the edge of the basal plane. These functionalities are described in Table 4.3 where the significant peaks from prior study are briefly presented.

Table 4.3: Infrared spectrum peaks for an interpretation of surface functional groups **[33]**.

IR peak bands [cm^{-1}]	**Implications**	**Chemical form**
~ 3200 - 3600	Corresponding to functional groups involved in H-bonding (N-H, O- H) ~ 3400 cm^{-1}: corresponding with hydroxyl groups (-OH) ~ 3600 cm^{-1}: corresponding with amine groups (-NH)	
~ 1650 - 1850	Corresponding to the functional groups consisting of the bonding C=O vibrations ~ 1830 cm^{-1}: five-membered ring lactone ~1737 cm^{-1}: five-membered ring lactone induced by hydroxyl groups ~ 1810 -1740 cm^{-1}: aldehyde ~ 1770 – 1670 cm^{-1}: aldehyde induced by hydroxyl groups ~1790 cm^{-1}: six-membered ring lactone ~ 1711 cm^{-1}: six-membered ring lactone induced by hydroxyl groups ~ 1750 cm^{-1}: carboxyl group	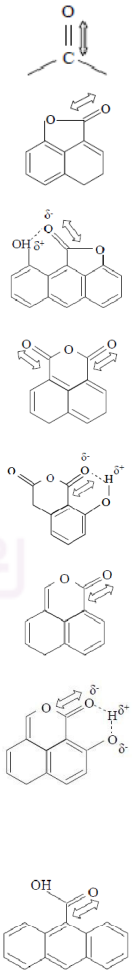

Table 4.3 (next): Infrared spectrum peaks for an interpretation of surface functional groups.

IR peak bands [cm^{-1}]	**Implications**	**Chemical form**
~ 1650 – 1850	~ 1660 – 1700 cm^{-1}: carboxyl group induced by hydroxyl groups	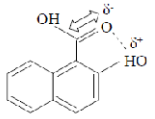
~ 1550 - 1650	Corresponding with C=C stretching vibration modes of the basal plane of activated carbons	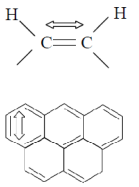
~1350 - 1550	Corresponding to C-H bending vibration mode in basal plane	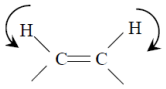
~ 1000 – 1300	Corresponding to C-O stretching vibration modes ~ 1025 – 1141 cm : cyclic ether group ~1230 – 1250 cm^{-1}: ether bridge between rings ~ 1160 – 1370 cm^{-1}: C-O in lactone ~ 980 – 1300 cm^{-1}: C-O in aldehyde ~ 1120 – 1200 cm^{-1}: C-O in carboxyl ~ 1160 – 1200 cm^{-1}: C-O-H bending vibration	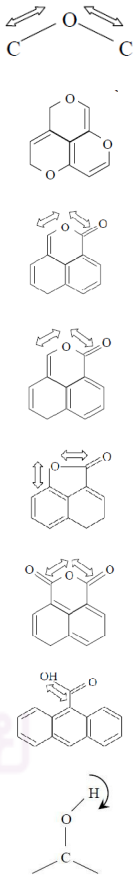
	~ 1000 – 1220 cm^{-1}: C-OH stretching vibration	
< 900	Corresponding to out-of-plane bending vibration of C-C in the basal plane of the activated carbon	

ศูนย์วิทยทรัพยากร
จุฬาลงกรณ์มหาวิทยาลัย

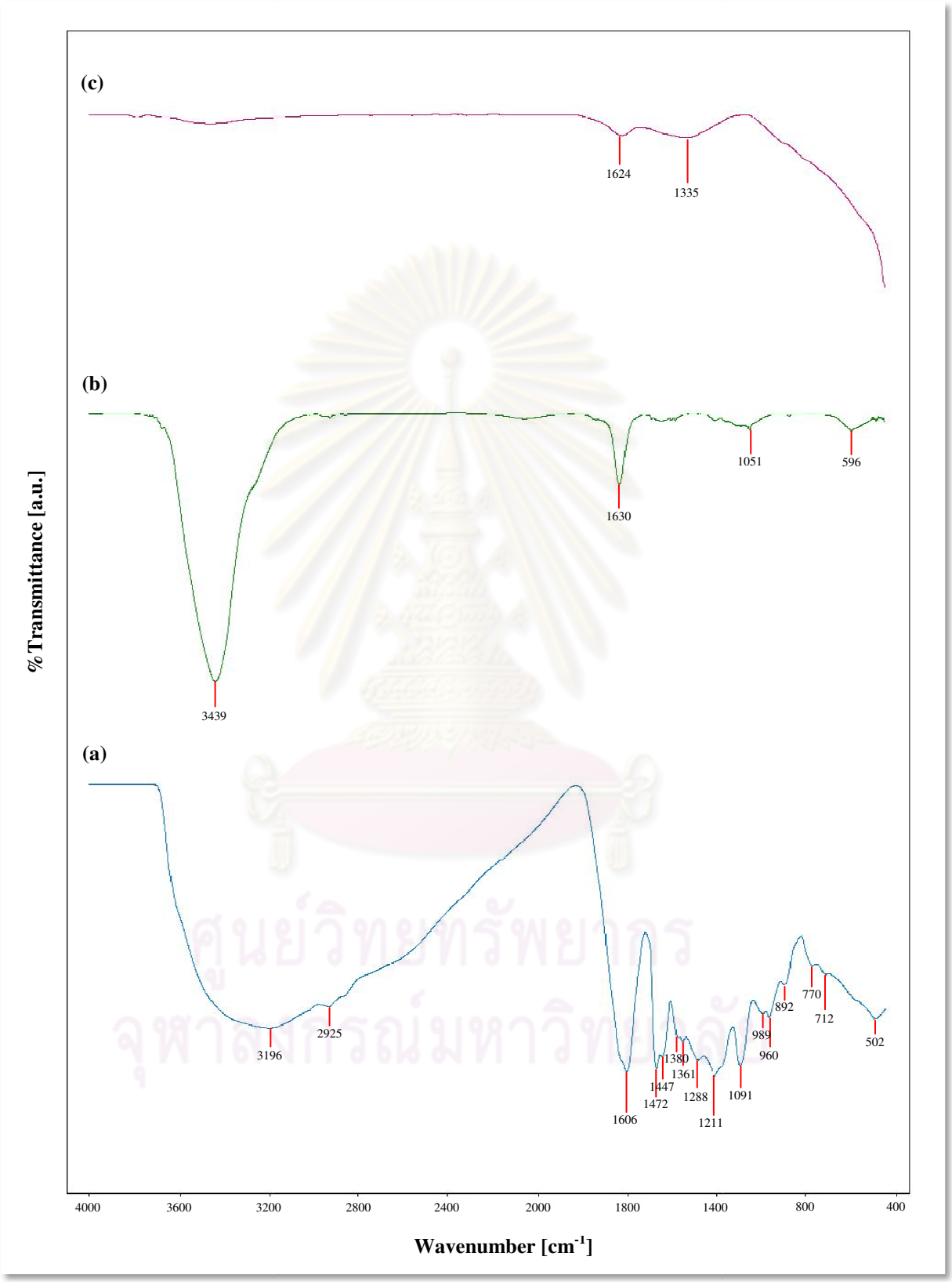

Figure 4.10 FTIR spectra of the RF monolith (a) and the carbon monolith obtained from thermal activation, C-CO_2 (b) and carbonization,C-N_2 (c).

The infrared spectra of RF monolith, carbon monolith conducted by thermal activation with CO_2 (C-CO_2) and carbon monolith prepared by carbonization with N_2 (C-N_2) are shown in Figure 4.10 (a), (b) and (c), respectively.

According to the Figure 4.10 (a), the infrared spectra of functional groups on surface of RF monolith are discussed. The peaks in range of 2800-3200 cm^{-1}, in this work at 3195 and 2935 cm^{-1} are assigned to C-H stretching and $–CH_2$ stretching in methylene bridge, respectively. The peak band at around 1606, 1472 and 1447 cm^{-1} can be attributed to the aromatic skeleton stretching. The peak in range of 1350-1500 cm^{-1} can be assigned to C-H bending vibration mode in basal plane. The peak at 1211, 1091 cm^{-1} can be ascribed to C-O-C linkage stretching between two resorcinol molecules. The peak at 1380 and 1361cm^{-1} can be attributed to phenolic-OH in plane deformation. The peak at 989 and 960 cm^{-1} correspond to out-of plane deformation vibrations of O-H groups monosubstituted to aromatic ring. The symmetric C-O-C is show the peak around at 892 cm^{-1}. The peak band below 850 cm^{-1} may be assigned to C-C out-of-plane binding at substituted positions in aromatic ring.

According to Figure 4.10 (b), there are four significant peaks can be observed at the peaks around 3439, 1630, 1051 and 586 cm^{-1}. The peak at 1630 and 586 cm^{-1}can be attribute to C=C stretching vibration modes and out-of –plane bending vibration of C-H , respectively, in the basal plane of carbon. The C-OH stretching vibration peak are showed in broad band at 1051 cm^{-1}. Moreover this peak is also attributed to the C-O-C stretching vibrations. Therefore, the present of peak at 3439 cm^{-1} can be assigned to the subsistence of hydroxyl or phenol group on the surface of carbon monolith.

From the Figure 4.10 (c), the infrared spectra of C-N_2 are considered. It is clear that there are only two peaks can be observed at all spectrum regions. The peak at 1624 and 1335 cm-1 can be attributed to C=C stretching vibration and C-H bending vibration modes in basal plane, respectively. Hence, there are not any function groups of oxygen on the surface of carbon monolith prepared by carbonization with N_2 as well as previous study [33].

In summary, the carbon monolith obtained by carbonization process has no functional group of oxygen on the surface while oxygen on the surface of carbon

monolith can be generated by thermal activation. The oxygenated surface is shown in Figure 4.11.

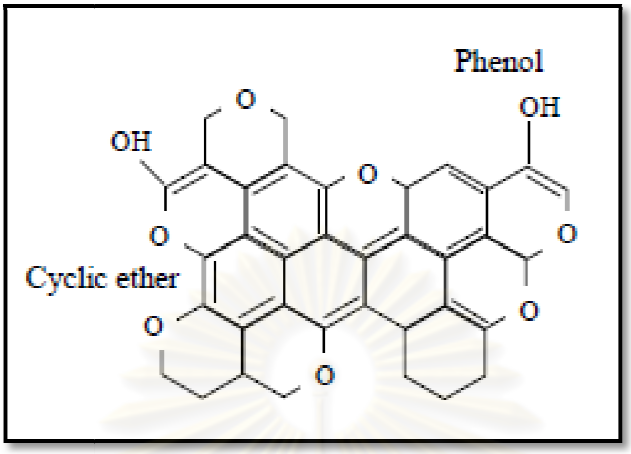

Figure 4.11 Possibly oxygenated function group of the carbon monolith prepared by thermal activation **[33]**

4.2 Optimal conditions for lipase immobilization on carbon RF gels

Carbon microbeads were used as supports for investigate the preparation conditions of enzyme solutions. The pH and ionic strength of phosphate buffer solutions were studied. In addition, the protein loading was also explained. The effects of these factors on immobilization of lipase were presented in this part.

4.2.1 The effect of pH on immobilization

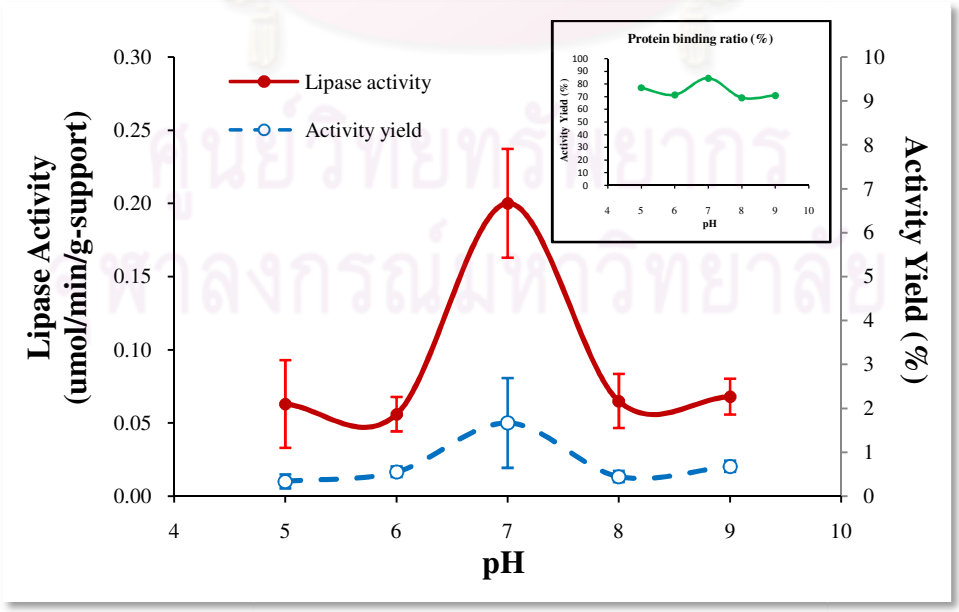

Figure 4.12 The effect of pH on the lipase activity and activity yield (%) of lipase immobilization at 20 mM ionic strength and 3 mg/ml protein loading

Lipase activity and activity yield at various reaction pH are presented in Figure 4.12. The highest activity of lipase (0.20 (±0.04) µmol/min/g-support) and activity yield (1.67 (±1.02) %) are obtained at pH 7. Correspondingly, the protein binding ratio is also the highest at this pH 7 which help promote enzyme activity. Thus, the optimal pH for preparation of enzyme solution is fixed at 7.

4.2.2 The effect of ionic strength on immobilization

When the optimal pH is obtained at 7, the concentrations of phosphate buffer solution are studied further at this pH. The effects of concentrations of phosphate buffer solutions on immobilized enzyme properties are shown in Figure 4.13. The highest lipase activity and activity yield are 0.20 (±0.04) µmol/min/g-support and 1.67 (±1.02) %, respectively obtained at phosphate buffer concentration of 20 mM. At the 20 mM phosphate buffer solutions, the protein binding ratio is also the highest value which may be the additional support reason for high activity besides the effect of pH.

The effect of ionic strength on lipase activity and the activity yield are shown in Figure 4.13, the proper ionic strength is s obtained at 20 mM.

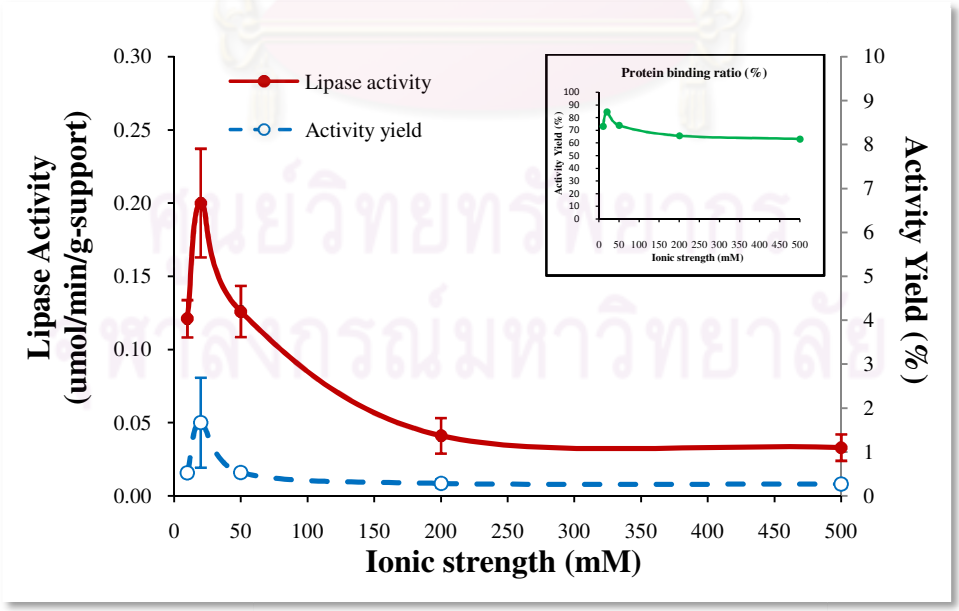

Figure 4.13 The effect of ionic strength on the lipase activity and activity yield (%) of lipase immobilization at pH 7 and 3 mg/ml protein loading

4.2.3 The effect of protein loading on immobilization

The protein loading are the last factor of preliminary conditions which performed in granule particle support form. It is studied in the range of 1-8 mg/ml at the suitable pH and ionic strength obtained from previous sections. From the Figure 4.14, the highest lipase activity and activity yield were obtained about 0.52 (±0.09) µmol/min/g-support and 21.02 (±3.15) %, respectively when 1 mg/ml protein loading was used. In contrast, the percent of protein binding ratio is lower than the others. From this result, it indicated that the highest activity does not depending on only the large amount of protein loading, but also on how well lipase on the support can function. It might be caused by shielding effect, steric impediments of immobilized lipase and the enzyme distributions on the support **[32]**. It is possible that the enzyme may induce high lipase activity at the low protein binding ratio. Hence, the optimal protein loading is used at 1 mg/ml.

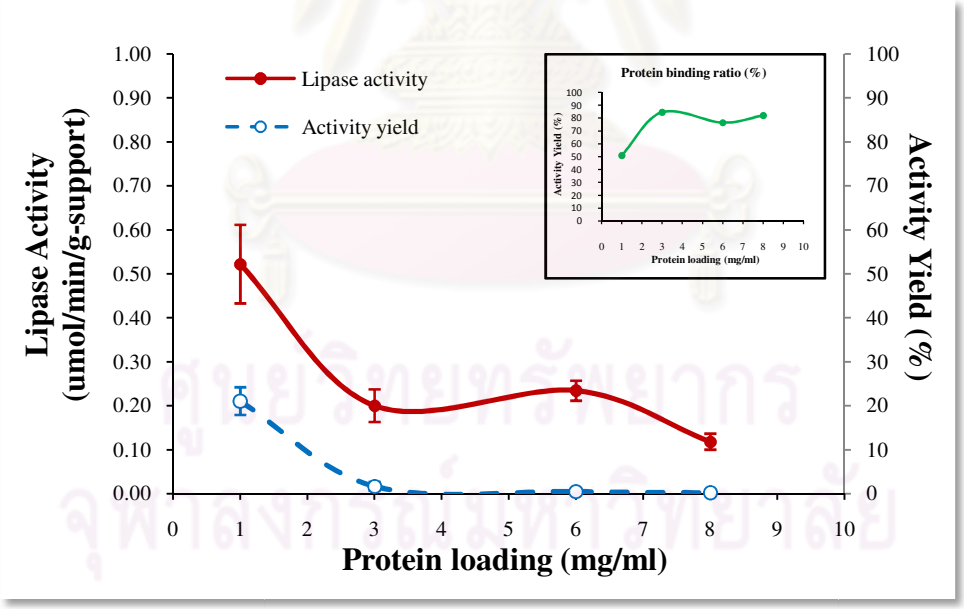

Figure 4.14 The effect of protein loading on the lipase activity and activity yield (%) of lipase immobilization at pH 7 and 20 mM ionic strength

4.3 Immobilization of *Candida rugosa* lipase on hierarchical porous carbon monoliths

The carbon monoliths with and without oxygen on surface were used for lipase immobilization by recirculation of enzyme solution method. The immobilization times and the flow rate of enzyme solution that effect on immobilization process were studied by using carbon monoliths with oxygen on surface (obtained from thermal activation). The kinetic parameters of two different characteristic of carbon monoliths were investigated.

4.3.1 The effect of immobilization times on residual activity of lipase

The decreasing tendency of residual lipase activity versus immobilization times are shown in Figure 4.15. It is found that the percent residual activities of lipase are rapidly decreased from initial time of incubation in few minutes and then constant after 10 minutes. Since the carbon monolith has a very large pore size compared with size of lipase, the enzymes easy rotate the hydrophobic site to attach with the surface inside the support. Moreover, by pumping the enzyme solutions into the column lipase can have more close contact throughout the supports. Thus, the optimal immobilizations for enzyme recirculation method are fixed at 2 hours to ensure that enzyme completely contact within the support.

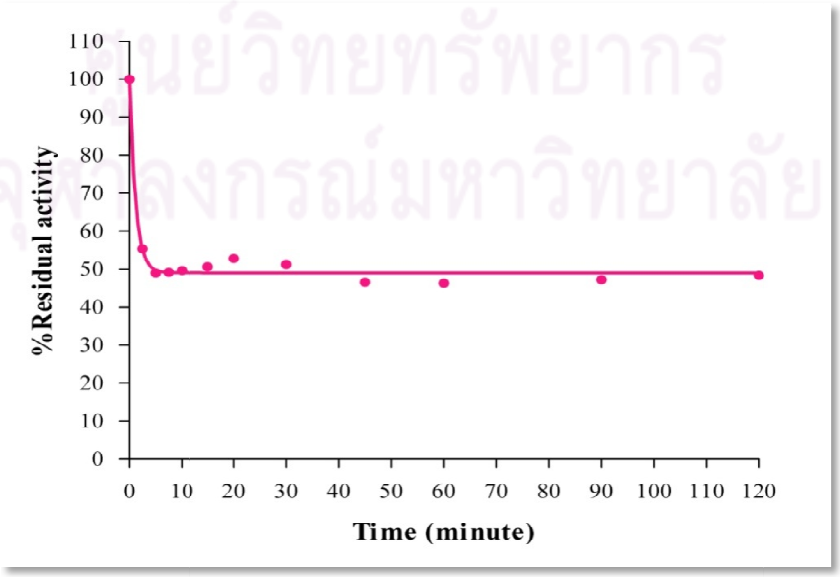

Figure 4.15 Residual activities at various immobilization times

4.3.2 The effect of flow rate on immobilization of lipase

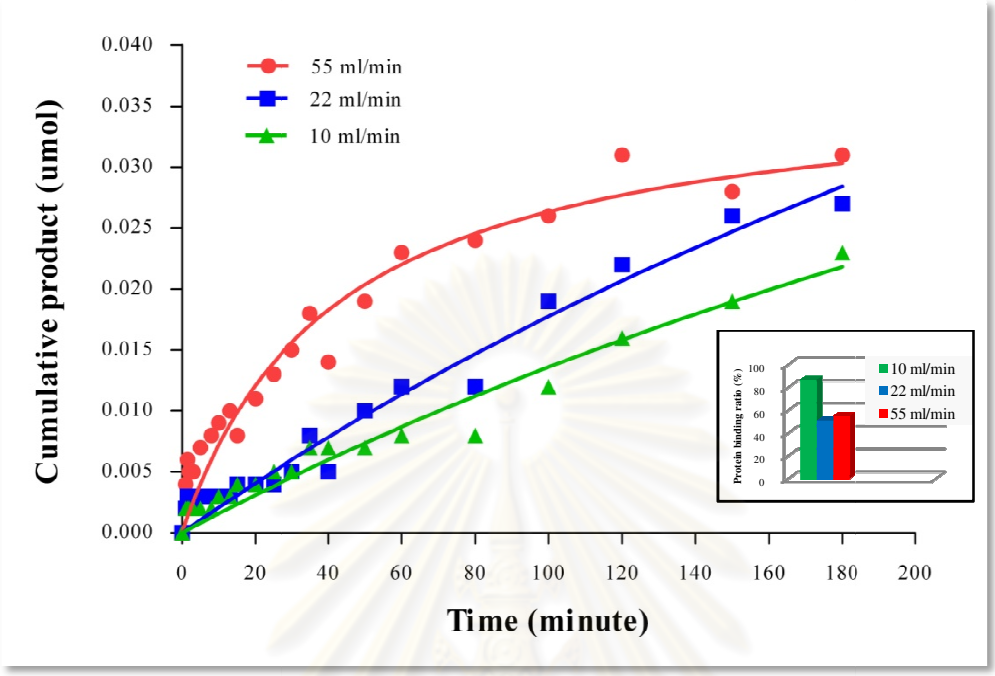

Figure 4.16 The effect of flow rate at recirculation of lipase solution in immobilization process on cumulative product at various reaction time

To study the effect of flow rate at recirculation of lipase solution in immobilization process on lipase activity. In this experiment, the lipase activity is measured in term of cumulative product. The results are shown in Figure 4.16.

According to Figure 4.16, it is indicated that the increase of flow rate of enzyme solution through the column packed porous carbon monolith led to significant raise of cumulative product.

At 55 ml/min flow rate, the fastest increase in the value of cumulative product are presented even if the protein binding ratio is lower than flow rate at 10 ml/min. For this result, the more protein loading at the 10 ml/min flow rate may provide enzyme more time to attach not only to enzyme and support, but also to enzyme and enzyme binding. Therefore, cumulative product slowly took place in the reaction since the effect of steric hindrance and enzyme distribution are dominant as mentioned in Section 4.2.3. When compare immobilization efficiency between flow rate of 55 and 22 ml/min, it can be seen that the protein binding ratio is slightly different. However, the higher increment of cumulative product at flow rate 55 ml/min was found. The initial rate of

reaction at flow rate 55 ml/min; 0.4 μmol/min, was much faster than 22 ml/min; 0.1 μmol/min, approximately 4-fold. Enzyme distribution within the support can be improved by high flow rate as well as proper ratio of enzyme to surface area. Therefore, the enzymes can fully function and the substrates can reach and react, easily.

4.3.3 Kinetic parameter of column packed hierarchical porous carbon monolith

In this section, kinetic parameter of the carbon monolith with (C-CO_2) and without (C-N_2) oxygen on surface are studied. Effects of oxygen on kinetic parameter such as kinetic constant (K_m for Michaelis-Menten equation and K'' for Boltzmann sigmoidal equation) and maximum velocity (V_{max}) of immobilized enzyme column reaction are investigated.

Table 4.4 Kinetic parameter of carbon monoliths

Type of column	Value from Graphpad Prism v.5			Protein binding ratio (%)
	Equation	K (mM)	V_{max} x 10^{-4} (μmol/min)	
C-CO_2	Michaelis-Menten	51.42	15.60	54.40
C-N_2	Boltzmann sigmoidal	25.67	8.32	49.82

The results of kinetic parameters of the column packed carbon monoliths are shown in Table 4.4. The initial velocities, V of the increase in the value cumulative product depending on the substrate concentration, [S], are measured. The results of C-CO_2 column is fitted to the Michaelis-Menten equation while C-N_2 column is analyzed by Boltzmann Sigmoidal equation. These results are evaluated by Graphpad Prism v.5.

According to Figure 4.17, graph of kinetic parameter of C-CO_2 and C-N_2 column are studied. The plots of V versus [S] fitted to Michaelis-Menten equation for C-CO_2 and Boltzmann sigmoidal equation for C-N_2 column are shown in Figure 4.17. From this figure, the result from C-CO_2 column indicates that an increase in the initial

velocity at lower substrate concentration, followed by gradual slope saturation is shown as well as a basic general enzyme-catalyzed reaction. The kinetic constant; affinity binding of enzyme toward substrate, K_m and the maximum velocity, V_{max} of C-CO_2 column are 51 mM and 1.56×10^{-3} µmol/min, respectively. In case of C-N_2, the result reveals that the initial velocity is slightly increased at low substrate concentration and then rapidly increases from 1.50×10^{-4} µmol/min to 7.00×10^{-4} µmol/min with increasing substrate concentration from 15 to 32 mM and the maximum velocity is obtained at approximately 8.32×10^{-4} µmol/min. The graph of C-N_2 column kinetic is indicated as sigmoidal curve which suggests *K"* of this column which is about 2 times lower than K_m from C-CO_2 column. This result indicates that C-N_2 column is less effective than C-CO_2 column. The sigmoidal curve might be cause from the solubility limit of the polar substrate in hydrophobic solvent. At low concentration of hydrophobic substrate, there is not enough substrate to fully function of all enzyme molecules because of higher lipase activity so the velocity of the reaction should be low whereas all molecules of enzyme are employed at high concentration therefore the enzymes are fully active giving normal distribution curve of single-substrate catalysis. Moreover, it still can be indicated that the immobilization of lipase on different functional group surface support can change the reaction mechanism of enzyme which normally enzyme single-substrate catalysis followed Michaelis-Menten equation is altered to sigmoidal equation.

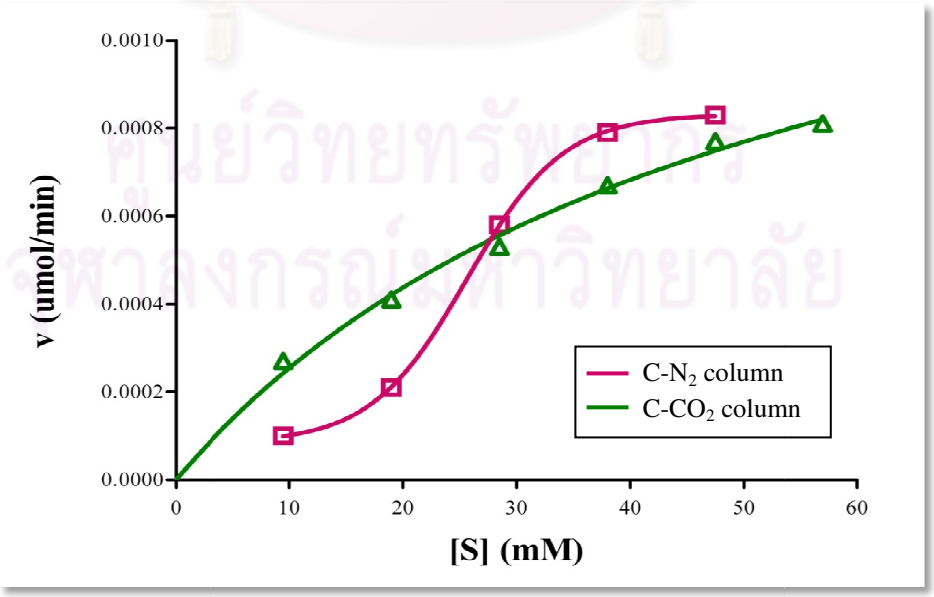

Figure 4.17 The kinetic behavior and parameters of C-CO_2 and C-N_2 column followed by Michaelis-Menten and Boltzmann sigmoidal equations, respectively

For the sigmoidal curve of C-N_2 column is possible that the immobilized lipase might be changed the oligomerization from monomeric form to dimeric form, which affects the catalytic mechanism. Only dimeric lipase has allosteric effect, which binding of the substrate in one subunit alter the affinity binding of substrate in nearby subunit. Dimerization of *C.rugosa* lipase has been reported in some type of surface support during enzyme immobilization. In addition, this sigmoidal curve is also might be cause of the limitation of diffusion and polarity of hydrophilic substrate. At lower substrate concentration, slower initial velocity was observed because of the limitation of diffusion. The substrate slowly diffuses to reach the enzyme **[34, 35]**. However, at high concentration of substrate, the reactant can overcome the diffusion limit so it does not affect the reaction. Moreover, the pore size and polarity of the support is also effect. It may possible that the pore size in the C-N_2 column is much larger compared with the size of lipase, at the low substrate concentration, the substrate has a slightly chance to contact the enzyme on surface. In addition, non polarity on the surface of C-N_2 prevents polar substrate from coming to react with the enzyme on the surface. However, oxygenated C-CO_2 column may improved the polarity on surface which can help the substrate ease to contact with the enzyme as well as showing in higher protein binding ratio in immobilization process.

Finally, this experiment confirmed that the different functional groups on surface and pore characteristic of the supports have significant effect on the reaction of immobilized enzyme. However, further experimental is needed to be studied.

ศูนย์วิทยทรัพยากร
จุฬาลงกรณ์มหาวิทยาลัย

CHAPTER V

CONCLUSIONS

All results in Chapter IV are concluded in this chapter which the subjects are divided into three parts. First, the conclusions of properties of the supports are described. Next, the results of optimal conditions that affect on the immobilization process are explained. Finally, immobilization of lipase on hierarchical porous carbon monolith with two different characteristics is summarized.

5.1 Properties of carbon supports

Physical properties of the carbon monoliths obtained from carbonization (C-CO_2) and thermal activation (C-N_2) are similar. The size and shape of C-N_2 are identical to C-CO_2 which the structure of these carbon monoliths can be maintained in monolith form after carbonization process. In addition, porosity of the two carbon monolith are slight different. It can be seen that the macropore skeleton in C-N_2 and C-CO_2 are almost the same. Macropore diameter and macropore volume of C-N_2 are slight larger than C-CO_2, but the micropore volume and S_{BET} of C-N_2 are smaller.

From the results of FTIR, it is indicated that the oxygen can be generated on surface of C-CO_2 after thermal activation process. Hence, the two carbon monoliths are different in functional group on surface within the porous structure.

5.2 Optimal conditions of lipase immobilization

There are many factors that have effect on the activity of lipase in immobilization process. For each supports used in immobilized lipase has different surface property. In this work, the basic important conditions for the first study are pH, ionic strength and protein loading. These factors are used in preparation of enzyme

solutions. The optimal pH, ionic strength and protein loading obtained from carbon bead supports are 7, 20 mM and 1mg/ml, respectively.

It is obviously seen that the pH and ionic strength of phosphate buffer solutions used for preparation of enzyme solutions promote close contact of enzyme on the surface inside the support as shown in high protein binding ratio. Furthermore, these factors may improve the enzyme activity. However, the results of the effect of protein loading reveal that the suitable amount of enzyme in the support are also significant since there is a high possibility that more protein loading in the support may cause steric impediment which leads to poor reaction of enzyme and substrate and results in low lipase activity. Finally, it is obviously seen that the protein loading has much more effect than pH and ionic strength.

5.3 The immobilization of lipase on column packed carbon monolith supports

In this parts, carbon monolith with (C-CO_2) and without (C-N_2) are used for immobilization of lipase. The immobilization times on recirculation enzyme solution technique is studied which the results indicated that enzyme are very fast come into the pores and attract on surface of the porous carbon support which result in rapidly decreasing of residual activity in few minutes as shown in Figure 4.15. However, the flow rate of enzyme solution is also affect on immobilization process. At the low flow rate of enzyme solution can help to improve the protein binding ratio because of enzyme has more time to attach not only to enzyme and support, but also to enzyme and enzyme binding, whereas the lipase activity is low since the steric impediment and low enzyme distribution. For high flow rate, the lipase show the binding limit observed from the protein binding ratios is slightly different at 22 ml/min and 55 ml/min. Moreover, the higher flow rate may improve the enzyme distribution result in the rapid increasing of cumulative product.

Finally, the kinetic behaviors of immobilized enzyme in the column are explained. It can be obviously seen that immobilization of lipase on different functional group surface support can change the reaction mechanism of enzyme which normally

enzyme single-substrate catalysis followed Michaelis-Menten equation is altered to sigmoidal equation. In case of immobilized enzyme in C-CO_2 column show the basic general enzyme-catalyzed reaction followed by Michaelis-Menten equation while immobilized enzyme in C-N_2 column show enzyme kinetic like a sigmoidal curve which might be cause from the solubility limit of the polar substrate in hydrophobic solvent. The C-N_2 column kinetic, *K"* is lower than K_m from C-CO_2 column which this result indicates that C-N_2 column is less effective than C-CO_2 column. Furthermore, oxygenated surface of C-CO_2 column can help to improve more protein binding ratio. However, more experimental data are needed for further investigation.

ศูนย์วิทยทรัพยากร
จุฬาลงกรณ์มหาวิทยาลัย

REFERENCES

[1] Ma, J., Zhang, L., Liang Z., Zhang, W., and Zhang, Y. Recent advances in immobilized enzymatic reactors and their applications in proteome analysis. Analytica Chimica Acta 632 (2009): 1–8.

[2] De Lathouder, K. M., Bakker, J.J.W., Kreutzer, M. T., Wallin, S. A., Kapteijn, F., and Moulijn, J.A. STRUCTURED REACTORS FOR ENZYME IMMOBILIZATION: A Monolithic Stirrer Reactor for Application in Organic Media. Chemical Engineering Research and Design 84 (2006): 390–398.

[3] Kumar, A.G., Swarnalatha, S., Kamatchi, P., Kirubagaran, R., Perinmbam, K., and Sekaran, G. Immobilization of proteolytic enzyme on highly porous activated carbon derived from rice bran. Journal of Porous Materials 16 (2008): 439-445.

[4] Kumar, A.G., Swarnalatha, S., Kamatchi, P., and Sekaran, G. Immobilization of high catalytic acid protease on functionalized mesoporous activated carbon particles. Biochemical Engineering Journal 43 (2009): 185–190.

[5] Andreescu, S., Njagi, J., and Ispas, C. Chaper 7: Nanostructured materials for enzyme immobilization and biosensors. Erokhin, V., Ram, K.M., and Yavuz, O., editors, The New Frontiers of Organic and Composite Nanotechnology, 355-394. London: Elsevier Science Publisher, 2007.

[6] Siyasukh, A., Maneeprom, P., Larpkiattaworn, S., Tonanon, N., Tanthapanichakoon, W., Tamon, H., and Charinpanitkul, T. Preparation of a carbon monolith with hierarchical porous structure by ultrasonic irradiation followed by carbonization, physical and chemical activation. Carbon 46 (2008): 1309-1315.

[7] Dizge, N., Aydiner, C., Imer, D.Y., Bayramoglu, M., Tanriseven, A., and Keskinler, B. Biodiesel production from sunflower, soybean, and waste

cooking oils by transesterification using lipase immobilized onto a novel microporous polymer. Bioresource Technology 100 (2008): 1983-1991.

[8] Leinweber F.C., and Tallarck, U. Chromatographic performance of monolithic and particulate stationary phase: hydrodynamic and adsorption capacity. Journal of Chromatography A 1006 (2003): 207–228.

[9] Macario, A., Moliner, M., Corma, A., and Giordano, G. Increasing stability and productivity of lipase enzyme by encapsulation in a porous organic–inorganic system. Microporous and Mesoporous Materials 118 (2009): 334–340.

[10] Santos, J.C., Mijone, P.D., Nunes, G.F.M., Perez, V.H., and de Castro, H.F. Covalent attachment of *Candida rugosa* lipase on chemically modified hybrid matrix of polysiloxane–polyvinyl alcohol with different activating compounds. Colloids and Surfaces B: Biointerfaces 61 (2008): 229–236.

[11] Tamon, H., and Ishizaka, H. Influence of Gelation Temperature and Catalysts on the Mesoporous Structure of Resorcinol–Formaldehyde Aerogels. Journal of Colloid and Interface Science 223 (2000): 305–307.

[12] Zubizarreta, L., Arenillas, A., Pirard, J.P., Pis, J.J., and Job, N. Tailoring the textural properties of activated carbon xerogels by chemical activation with KOH. Microporous and Mesoporous Materials 115 (2008): 480-490.

[13] Yamamoto, T., Nishimura, T., Suzuki T., and Tamon, H. Effect of drying conditions on mesoporosity of carbon precursors prepared by sol–gel polycondensation and freeze drying. Carbon 39 (2001): 2369 –2386.

[14] Lin, C., and Ritter, J.A. Effect of synthesis pH on the structure of carbon xerogels. Carbon 35 (1997): 1271-1278.

[15] Yamamoto, T., Mukai, S.R., Endo, A., Nakaiwa, M., and Tamon, H. Interpretation of structure formation during the sol-gel transition of a resorcinol-formaldehyde solution by population balance. Journal of Colloid and Interface Science 264 (2003): 532–537.

[16] Pekala, R.W. Organic aerogels from the polycondensation of resorcinol with formaldehyde. Journal of materials 24 (1989): 3221-3227.

[17] Pahl, R., Bonser, U., Pekala, R.W., and Kinney, J.H. SAXS Investigations on Organic Aerogels. Journal of Applied Crystallography 24 (1991): 771-776.

[18] Yamamoto, T., Yoshida, T., Suzuki, T., Mukai, S.R., and Tamon, H. Dynamic and Static Light Scattering Study on the Sol-Gel Transition of Resorcinol-Formaldehyde Aqueous Solution. Journal of Colloid and Interface Science 245 (2002): 391–396.

[19] Yamamoto, T., Nishimura, T., Suzuki, T., and Tamon, H. Effect of drying method on mesoporosity of resorcinol-formaldehyde drygel and carbon gel. Drying Technology 19(7) (2001): 1319–1333.

[20] Gommes, C.J., Job, N., Pirard, J.P., Blacher, S., and Goderis, B. Critical opalescence points to thermodynamic instability: relevance to small-angle X-ray scattering of resorcinol–formaldehyde gel formation at low pH. Journal of Applied Crystallography 41 (2008): 663-668.

[21] Nakanishi, K., Minakuchi, H., and Soga, N. Double pore silica gel monolith applied to liquid chromatography. Journal of Sol-Gel Science and Technology 8 (1997): 547–552.

[22] Ikegami, T., and Tanaka, N. Monolithic columns for high-efficiency HPLC separations. Current Opinion in Chemical Biology 8 (2004): 527–33.

[23] Fuchigami, T., Toki, M., and Nakanishi, K. Membrane emulsification using sol–gel derived macroporous silica glass. Journal of Sol-Gel Science and Technology 19 (2000): 337–341.

[24] Chen, S.X., Zhang, X., and Shen, P.K. Macroporous conducting matrix: fabrication and application as electrocatalyst support. Electrochemistry Communications 8 (2008): 713-719.

[25] Pernas, M.A., Lopez, C., Luisa Rua, M., and Hermoso, J. Influence of the conformational flexibility on the kinetics and dimerisation process of two Candida rugosa lipase isoenzymes. FEBS Letters 501 (2001): 87-91.

[26] Reis, P., Holmberg, K., and Watzke, H., Leser, M.E., and Miller,R. Lipases at interfaces: A review. Advances in Colloid and Interface Science 147–148 (2009): 237–250.

[27] Supaluk Tantong. Optimal conditions for the covalent immobilization of lipase from *Candida rugosa* for the production of biodiesel. Thesis for the Degree of Master of Science Program in Biotechnology, Faculty of Science, Chulalongkorn University, 2008.

[28] Cygler, M., and Schrag, J.D. Structure and conformational flexibility of Candida rugosa lipase. Biochimica et Biophysica Acta 1441 (1999): 205-214.

[29] De Maria, P.D., Sanchez-Montero, J.M., Sinisterra, J.V., and Alcantara, A.R. Understanding Candida rugosa lipases: An overview. Biotechnology Advances 24 (2006): 180– 196.

[30] Tischer, W., and Wedekind, F. Immobilized Enzymes: Methods and Applications. Topics in Current Chemistry, Vol 200: 95-126. Berlin: Springer Berlin/Heidelberg Publisher, 1999.

[31] Chaijitrsakool, T., Tonanon, N., Tanthapanichakoon, W., Tamon, H., and Prichanont, S. Effects of pore characters of mesoporous resorcinol–formaldehyde carbon gels on enzyme immobilization. Journal of Molecular Catalysis B: Enzymatic 55 (2008): 137–141.

[32] Shakeri, M., and Kawakami, K. Effect of the structural chemical composition of mesoporous materials on the adsorption and activation of the Rhizopus oryzae lipase-catalyzed trans-esterification reaction in organic solvent. Catalysis Communications 10 (2008): 165–168.

[33] Adisak Siyasukh. Preparation of hierarchical porous carbon monolith without using templates. Dissertation the Degree of Doctor of Engineering Program in Chemical Engineering, Department of Chemical Engineering, Faculty of Engineering, Chulalongkorn University, 2008.

[34] Mateo, C., Palomo, J.M., Fernandez-Lorente, G., Guisan, J.M., and Fernandez-Lafuente, R. Improvement of enzyme activity, stability and selectivity via immobilization techniques. Enzyme and Microbial Technology 40 (2007): 1451–1463.

[35] Kato, M., Inuzuka, K., Sakai-Kato, K., and Toyo'oka, T. Monolithic Bioreactor Immobilizing Trypsin for High-Throughput Analysis. Analytical Chemistry 77 (2005): 1813-1818.

[36] Chang, S.F., Chang, S.W., Yen, Y.H. and Sheih, C.J. Optimum immobilization of Candida rugosa lipase on Celite by RSM. Applied Clay Science 37 (2007): 67-73.

[37] Kingkaew Piriyakananon. Optimal immobilization conditions of lipase from *Candida rugosa* for biodiesel production. Thesis for the Degree of Master of Science Program in Biotechnology, Faculty of Science, Chulalongkorn University, 2009.

[38] Nicoli, R., Gaud, N., Stella, C., Rudaz, S., and Veuthey, J.L. Trypsin immobilization on three monolithic disks for on-line protein digestion. Journal of Pharmaceutical and Biomedical Analysis 48 (2008): 398–407.

[39] Gargouri, M., and Legoy, M.D. The kinetic behaviour of a two-enzyme system in biphasic media: coupling hydrolysis and lipoxygenation. Biochimica et Biophysica Acta 1337 (1997): 227–232.

ศูนย์วิทยทรัพยากร
จุฬาลงกรณ์มหาวิทยาลัย

APPENDICES

ศูนย์วิทยทรัพยากร
จุฬาลงกรณ์มหาวิทยาลัย

APPENDIX A

Properties of supports

A.1 Macropore size distribution

Table A-1 Pore size distribution by volume of C-CO_2

Pore diameter (μm)	Delta volume (cm^3/g)	Cumulative volume (cm^3/g)	Pore diameter (μm)	Delta volume (cm^3/g)	Cumulative Volume (cm^3/g)
2.187E+02	0.0000	0.0000	2.124E+01	0.0018	0.0255
1.706E+02	0.0032	0.0032	2.051E+01	0.0020	0.0275
1.431E+02	0.0014	0.0046	1.920E+01	0.0031	0.0330
1.212E+02	0.0010	0.0056	1.861E+01	0.0041	0.0371
1.046E+02	0.0008	0.0064	1.806E+01	0.0054	0.0425
9.202E+01	0.0007	0.0071	1.754E+01	0.0073	0.0498
8.190E+01	0.0010	0.0081	1.705E+01	0.0098	0.0596
7.370E+01	0.0006	0.0087	1.660E+01	0.0130	0.0726
6.663E+01	0.0006	0.0093	1.617E+01	0.0167	0.0893
6.053E+01	0.0006	0.0099	1.576E+01	0.0212	0.1105
5.548E+01	0.0006	0.0105	1.537E+01	0.0254	0.1359
5.104E+01	0.0006	0.0111	1.501E+01	0.0293	0.1652
4.728E+01	0.0005	0.0116	1.466E+01	0.0320	0.1972
4.391E+01	0.0006	0.0122	1.434E+01	0.0326	0.2298
4.100E+01	0.0006	0.0128	1.404E+01	0.0342	0.2640
3.835E+01	0.0006	0.0134	1.375E+01	0.0349	0.2989
3.613E+01	0.0006	0.0140	1.349E+01	0.0338	0.3327
3.424E+01	0.0006	0.0146	1.324E+01	0.0322	0.3649
3.263E+01	0.0006	0.0152	1.301E+01	0.0304	0.3953
3.116E+01	0.0006	0.0158	1.279E+01	0.0280	0.4233
2.981E+01	0.0007	0.0165	1.257E+01	0.0243	0.4476
2.857E+01	0.0006	0.0171	1.236E+01	0.0209	0.4685
2.743E+01	0.0007	0.0178	1.216E+01	0.0180	0.4865
2.639E+01	0.0007	0.0185	1.197E+01	0.0159	0.5024
2.541E+01	0.0008	0.0193	1.177E+01	0.0151	0.5175
2.451E+01	0.0008	0.0201	1.158E+01	0.0129	0.5304
2.366E+01	0.0010	0.0211	1.140E+01	0.0110	0.5414
2.283E+01	0.0012	0.0223	1.121E+01	0.0101	0.5515
2.202E+01	0.0014	0.0237	1.103E+01	0.0091	0.5606

Pore diameter (µm)	Delta volume (cm^3/g)	Cumulative volume (cm^3/g)	Pore diameter (µm)	Delta volume (cm^3/g)	Cumulative Volume (cm^3/g)
1.085E+01	0.0075	0.5681	4.122E-02	0.0000	0.6308
1.068E+01	0.0060	0.5741	3.947E-02	0.0000	0.6308
1.052E+01	0.0050	0.5791	3.785E-02	0.0000	0.6308
9.927E+00	0.0039	0.5830	3.634E-02	0.0000	0.6308
8.324E+00	0.0027	0.5887	3.494E-02	0.0000	0.6308
7.219E+00	0.0034	0.5921	3.364E-02	0.0000	0.6308
5.928E+00	0.0038	0.5959	3.242E-02	0.0000	0.6308
4.613E+00	0.0039	0.5998	3.127E-02	0.0000	0.6308
3.391E+00	0.0040	0.6038	3.020E-02	0.0000	0.6308
2.386E+00	0.0039	0.6077	2.919E-02	0.0000	0.6308
1.650E+00	0.0039	0.6116	2.824E-02	0.0000	0.6308
1.160E+00	0.0039	0.6155	2.734E-02	0.0000	0.6308
8.378E-01	0.0039	0.6194	2.649E-02	0.0000	0.6308
6.260E-01	0.0037	0.6231	2.569E-02	0.0000	0.6308
4.805E-01	0.0033	0.6264	2.493E-02	0.0000	0.6308
3.784E-01	0.0026	0.6290	2.421E-02	0.0000	0.6308
3.048E-01	0.0012	0.6302	2.352E-02	0.0000	0.6308
2.504E-01	0.0005	0.6307	2.287E-02	0.0000	0.6308
2.095E-01	0.0001	0.6308	2.224E-02	0.0000	0.6308
1.783E-01	0.0000	0.6308	2.165E-02	0.0000	0.6308
1.542E-01	0.0000	0.6308	2.108E-02	0.0000	0.6308
1.353E-01	0.0000	0.6308	2.054E-02	0.0000	0.6308
1.203E-01	0.0000	0.6308	2.002E-02	0.0000	0.6308
1.081E-01	0.0000	0.6308	1.953E-02	0.0000	0.6308
9.796E-02	0.0000	0.6308	1.905E-02	0.0000	0.6308
8.963E-02	0.0000	0.6308	1.860E-02	0.0000	0.6308
8.253E-02	0.0000	0.6308	1.816E-02	0.0000	0.6308
7.646E-02	0.0000	0.6308	1.774E-02	0.0000	0.6308
7.117E-02	0.0000	0.6308	1.734E-02	0.0000	0.6308
6.653E-02	0.0000	0.6308	1.695E-02	0.0000	0.6308
6.242E-02	0.0000	0.6308	1.658E-02	0.0000	0.6308
5.876E-02	0.0000	0.6308	1.622E-02	0.0000	0.6308
5.548E-02	0.0000	0.6308	1.587E-02	0.0000	0.6308
5.253E-02	0.0000	0.6308	1.553E-02	0.0000	0.6308
4.986E-02	0.0000	0.6308	1.520E-02	0.0000	0.6308
4.743E-02	0.0000	0.6308	1.489E-02	0.0000	0.6308
4.519E-02	0.0000	0.6308	1.457E-02	0.0000	0.6308
4.313E-02	0.0000	0.6308	1.426E-02	0.0000	0.6308

Pore diameter (μm)	Delta volume (cm^3/g)	Cumulative volume (cm^3/g)	Pore diameter (μm)	Delta volume (cm^3/g)	Cumulative Volume (cm^3/g)
1.397E-02	0.0000	0.6308	6.607E-03	0.0000	0.6308
1.368E-02	0.0000	0.6308	6.537E-03	0.0000	0.6308
1.340E-02	0.0000	0.6308	6.508E-03	0.0000	0.6308
1.313E-02	0.0000	0.6308			
1.287E-02	0.0000	0.6308			
1.262E-02	0.0000	0.6308			
1.238E-02	0.0000	0.6308			
1.215E-02	0.0000	0.6308			
1.193E-02	0.0000	0.6308			
1.171E-02	0.0000	0.6308			
1.151E-02	0.0000	0.6308			
1.131E-02	0.0000	0.6308			
1.112E-02	0.0000	0.6308			
1.094E-02	0.0000	0.6308			
1.076E-02	0.0000	0.6308			
1.058E-02	0.0000	0.6308			
1.041E-02	0.0000	0.6308			
1.025E-02	0.0000	0.6308			
1.008E-02	0.0000	0.6308			
9.925E-03	0.0000	0.6308			
9.772E-03	0.0000	0.6308			
9.624E-03	0.0000	0.6308			
9.481E-03	0.0000	0.6308			
9.341E-03	0.0000	0.6308			
9.204E-03	0.0000	0.6308			
9.070E-03	0.0000	0.6308			
8.940E-03	0.0000	0.6308			
7.477E-03	0.0000	0.6308			
7.380E-03	0.0000	0.6308			
7.285E-03	0.0000	0.6308			
7.192E-03	0.0000	0.6308			
7.101E-03	0.0000	0.6308			
7.011E-03	0.0000	0.6308			
6.924E-03	0.0000	0.6308			
6.845E-03	0.0000	0.6308			
6.763E-03	0.0000	0.6308			
6.683E-03	0.0000	0.6308			

Table A-2 Pore size distribution by volume of C-N_2

Pore diameter (µm)	Delta volume (cm^3/g)	Cumulative Volume (cm^3/g)	Pore diameter (µm)	Delta volume (cm^3/g)	Cumulative Volume (cm^3/g)
2.415E+02	0.0000	0.0000	1.606E+01	0.0273	0.5220
1.689E+02	0.0046	0.0046	1.564E+01	0.0228	0.5448
1.274E+02	0.0038	0.0084	1.486E+01	0.0148	0.5778
1.028E+02	0.0030	0.0114	1.450E+01	0.0121	0.5899
8.660E+01	0.0023	0.0137	1.416E+01	0.0098	0.5997
7.500E+01	0.0019	0.0156	1.384E+01	0.0080	0.6077
6.610E+01	0.0025	0.0181	1.353E+01	0.0064	0.6141
5.908E+01	0.0020	0.0201	1.325E+01	0.0051	0.6192
5.347E+01	0.0019	0.0220	1.299E+01	0.0037	0.6229
4.890E+01	0.0018	0.0238	1.275E+01	0.0023	0.6252
4.509E+01	0.0017	0.0255	1.252E+01	0.0013	0.6265
4.184E+01	0.0019	0.0274	1.231E+01	0.0007	0.6272
3.905E+01	0.0023	0.0297	1.211E+01	0.0005	0.6277
3.661E+01	0.0025	0.0322	1.192E+01	0.0003	0.6280
3.445E+01	0.0030	0.0352	1.175E+01	0.0002	0.6282
3.254E+01	0.0037	0.0389	1.158E+01	0.0002	0.6284
3.083E+01	0.0047	0.0436	1.141E+01	0.0001	0.6285
2.928E+01	0.0063	0.0499	1.125E+01	0.0001	0.6286
2.795E+01	0.0071	0.0570	1.110E+01	0.0000	0.6286
2.679E+01	0.0080	0.0650	1.060E+01	0.0001	0.6287
2.577E+01	0.0091	0.0741	9.864E+00	0.0001	0.6288
2.482E+01	0.0118	0.0859	8.718E+00	0.0005	0.6293
2.394E+01	0.0154	0.1013	7.129E+00	0.0010	0.6303
2.311E+01	0.0196	0.1209	5.261E+00	0.0013	0.6316
2.235E+01	0.0242	0.1451	3.556E+00	0.0014	0.6330
2.163E+01	0.0285	0.1736	2.329E+00	0.0015	0.6345
2.096E+01	0.0326	0.2062	1.546E+00	0.0015	0.6360
2.033E+01	0.0350	0.2412	1.066E+00	0.0015	0.6375
1.974E+01	0.0360	0.2772	7.651E-01	0.0015	0.6390
1.915E+01	0.0376	0.3148	5.696E-01	0.0015	0.6405
1.857E+01	0.0385	0.3533	4.383E-01	0.0014	0.6419
1.801E+01	0.0387	0.3920	3.464E-01	0.0014	0.6433
1.747E+01	0.0371	0.4291	2.802E-01	0.0010	0.6443
1.697E+01	0.0344	0.4635	2.313E-01	0.0005	0.6448
1.650E+01	0.0312	0.4947	1.946E-01	0.0001	0.6449

Pore diameter (μm)	Delta volume (cm^3/g)	Cumulative Volume (cm^3/g)	Pore diameter (μm)	Delta volume (cm^3/g)	Cumulative Volume (cm^3/g)
1.667E-01	0.0001	0.6450	2.096E-02	0.0000	0.6450
1.452E-01	0.0000	0.6450	2.042E-02	0.0000	0.6450
1.284E-01	0.0000	0.6450	1.991E-02	0.0000	0.6450
1.149E-01	0.0000	0.6450	1.942E-02	0.0000	0.6450
9.464E-02	0.0000	0.6450	1.895E-02	0.0000	0.6450
8.690E-02	0.0000	0.6450	1.850E-02	0.0000	0.6450
8.028E-02	0.0000	0.6450	1.807E-02	0.0000	0.6450
7.455E-02	0.0000	0.6450	1.765E-02	0.0000	0.6450
6.954E-02	0.0000	0.6450	1.723E-02	0.0000	0.6450
6.513E-02	0.0000	0.6450	1.683E-02	0.0000	0.6450
6.121E-02	0.0000	0.6450	1.645E-02	0.0000	0.6450
5.710E-02	0.0000	0.6450	1.607E-02	0.0000	0.6450
5.454E-02	0.0000	0.6450	1.571E-02	0.0000	0.6450
5.169E-02	0.0000	0.6450	1.535E-02	0.0000	0.6450
4.908E-02	0.0000	0.6450	1.500E-02	0.0000	0.6450
4.671E-02	0.0000	0.6450	1.466E-02	0.0000	0.6450
4.452E-02	0.0000	0.6450	1.433E-02	0.0000	0.6450
4.252E-02	0.0000	0.6450	1.401E-02	0.0000	0.6450
4.068E-02	0.0000	0.6450	1.371E-02	0.0000	0.6450
3.897E-02	0.0000	0.6450	1.343E-02	0.0000	0.6450
3.739E-02	0.0000	0.6450	1.316E-02	0.0000	0.6450
3.592E-02	0.0000	0.6450	1.289E-02	0.0000	0.6450
3.455E-02	0.0000	0.6450	1.264E-02	0.0000	0.6450
3.327E-02	0.0000	0.6450	1.240E-02	0.0000	0.6450
3.208E-02	0.0000	0.6450	1.217E-02	0.0000	0.6450
3.096E-02	0.0000	0.6450	1.195E-02	0.0000	0.6450
2.991E-02	0.0000	0.6450	1.175E-02	0.0000	0.6450
2.892E-02	0.0000	0.6450	1.154E-02	0.0000	0.6450
2.799E-02	0.0000	0.6450	1.135E-02	0.0000	0.6450
2.711E-02	0.0000	0.6450	1.116E-02	0.0000	0.6450
2.628E-02	0.0000	0.6450	1.097E-02	0.0000	0.6450
2.549E-02	0.0000	0.6450	1.079E-02	0.0000	0.6450
2.474E-02	0.0000	0.6450	1.062E-02	0.0000	0.6450
2.403E-02	0.0000	0.6450	1.044E-02	0.0000	0.6450
2.336E-02	0.0000	0.6450	1.028E-02	0.0000	0.6450
2.271E-02	0.0000	0.6450	1.012E-02	0.0000	0.6450
2.210E-02	0.0000	0.6450	9.959E-03	0.0000	0.6450
2.152E-02	0.0000	0.6450	9.808E-03	0.0000	0.6450

Pore diameter (μm)	Delta volume (cm^3/g)	Cumulative Volume (cm^3/g)	Pore diameter (μm)	Delta volume (cm^3/g)	Cumulative Volume (cm^3/g)
9.660E-03	0.0001	0.6451			
9.516E-03	0.0001	0.6452			
9.376E-03	0.0001	0.6453			
9.239E-03	0.0001	0.6454			
9.106E-03	0.0002	0.6456			
8.975E-03	0.0002	0.6458			
8.848E-03	0.0002	0.6460			
8.724E-03	0.0003	0.6463			
8.602E-03	0.0003	0.6466			
8.482E-03	0.0003	0.6469			
8.364E-03	0.0003	0.6472			
8.248E-03	0.0005	0.6477			
8.136E-03	0.0005	0.6482			
8.025E-03	0.0004	0.6486			
7.917E-03	0.0004	0.6490			
7.811E-03	0.0004	0.6494			
7.707E-03	0.0004	0.6498			
7.606E-03	0.0005	0.6503			
7.507E-03	0.0004	0.6507			
7.409E-03	0.0004	0.6511			
7.314E-03	0.0004	0.6515			
7.221E-03	0.0003	0.6518			
7.129E-03	0.0001	0.6519			
7.039E-03	0.0001	0.6520			
6.951E-03	0.0001	0.6521			
6.865E-03	0.0001	0.6522			
6.781E-03	0.0002	0.6524			
6.699E-03	0.0000	0.6524			
6.618E-03	0.0000	0.6524			
6.539E-03	0.0000	0.6524			
6.461E-03	0.0002	0.6526			

A.2 Size distribution of carbon beads

Table A-3 Size distribution by volume of C-N_2

Size (μm)	Vol. in %	Size (μm)	Vol. in %	Size (μm)	Vol. in %
0.01	0.00	2.05	0.11	389.97	0.01
0.01	0.00	2.35	0.11	447.75	0.00
0.01	0.00	2.70	0.09	514.09	0.00
0.02	0.00	3.10	0.08	590.25	0.00
0.02	0.00	3.56	0.02	677.70	0.00
0.02	0.00	4.08	0.00	778.10	0.00
0.02	0.00	4.69	0.00	893.38	0.00
0.03	0.00	5.38	0.00	1025.74	0.00
0.03	0.00	6.18	0.00	1177.70	0.00
0.04	0.00	7.10	0.00	1352.18	0.00
0.04	0.00	8.15	0.00	1552.51	0.00
0.05	0.00	9.36	0.00	1782.52	0.00
0.06	0.00	10.74	0.00	2046.61	0.00
0.06	0.00	12.33	0.00	2349.82	0.00
0.07	0.00	14.16	0.00	2697.96	0.00
0.09	0.00	16.26	0.00	3097.67	0.00
0.10	0.00	18.67	0.00	3556.60	0.00
0.11	0.00	21.43	0.00	4083.53	0.00
0.13	0.00	24.61	0.00	4688.52	0.00
0.15	0.00	28.25	0.00	5383.14	0.00
0.17	0.00	32.44	0.05	6180.67	0.00
0.20	0.00	37.24	0.61	7096.36	0.00
0.22	0.00	42.76	1.73	8147.71	0.00
0.26	0.00	49.10	3.43	9354.82	0.00
0.30	0.00	56.37	5.60		
0.34	0.00	64.72	7.98		
0.39	0.00	74.31	10.16		
0.45	0.00	85.32	11.74		
0.51	0.00	97.96	12.36		
0.59	0.04	112.47	11.91		
0.68	0.06	129.13	10.52		
0.78	0.07	148.26	8.47		
0.89	0.07	170.23	6.21		
1.03	0.07	195.45	4.06		
1.18	0.08	224.41	2.36		
1.35	0.08	257.65	1.15		
1.55	0.09	295.83	0.46		
1.78	0.10	339.65	0.10		

A.3 N_2 Adsorption-Desorption Isotherm

Table A-4 N_2 Adsorption-Desorption Isotherm at 77K of C-CO_2 monolith

Adsorption		Desorption	
p/p_0	V_a/cm^3(STP) g^{-1}	p/p_0	V_a/cm^3(STP) g^{-1}
4.004E-05	22.95	9.768E-01	186.10
4.003E-05	52.90	9.260E-01	174.95
1.201E-04	82.82	9.032E-01	173.55
4.801E-04	112.36	8.528E-01	171.73
2.001E-03	124.08	7.965E-01	170.60
4.039E-03	129.76	7.444E-01	169.85
6.796E-03	133.54	6.930E-01	169.22
1.974E-02	141.12	6.431E-01	168.67
2.760E-02	143.36	5.927E-01	168.13
3.893E-02	145.68	5.430E-01	167.57
5.175E-02	147.50	4.957E-01	166.80
8.077E-02	150.42	4.465E-01	165.76
1.092E-01	152.49	3.999E-01	164.33
1.354E-01	154.01	3.482E-01	163.01
1.616E-01	155.31	2.985E-01	161.67
1.869E-01	156.45	2.727E-01	160.90
2.124E-01	157.54	2.480E-01	160.12
2.381E-01	158.52	2.231E-01	159.29
2.636E-01	159.41	1.987E-01	158.44
2.891E-01	160.26	1.742E-01	157.50
3.141E-01	161.08	1.495E-01	156.48
3.599E-01	162.38	1.255E-01	155.36
4.068E-01	163.53	1.016E-01	154.05
4.584E-01	164.61		
5.093E-01	165.50		
5.598E-01	166.28		
6.105E-01	166.97		
6.607E-01	167.59		
7.106E-01	168.24		
7.603E-01	168.89		
8.090E-01	169.65		
8.577E-01	170.61		
9.040E-01	172.04		
9.500E-01	175.61		
9.743E-01	182.30		
9.914E-01	206.03		

Table A-5 N_2 Adsorption-Desorption Isotherm at 77 K of C-N_2 monolith

Adsorption		Desorption	
p/p_0	V_a/cm^3(STP) g^{-1}	p/p_0	V_a/cm^3(STP) g^{-1}
3.892E-04	22.10	9.401E-01	125.42
6.040E-04	45.76	8.856E-01	125.43
1.290E-03	64.46	8.366E-01	125.42
3.760E-03	83.11	7.860E-01	125.45
1.484E-02	100.67	7.367E-01	125.44
4.885E-02	112.20	6.869E-01	125.40
7.441E-02	114.15	6.376E-01	125.30
9.703E-02	115.84	5.908E-01	124.90
1.374E-01	117.80	5.384E-01	124.63
1.591E-01	118.68	4.872E-01	124.53
1.907E-01	119.37	4.376E-01	124.43
2.110E-01	119.82	3.880E-01	124.30
2.420E-01	120.30	3.384E-01	124.12
2.613E-01	120.65	2.890E-01	123.88
2.941E-01	121.02	2.679E-01	123.76
3.073E-01	121.32	2.426E-01	123.59
3.536E-01	121.81	2.183E-01	123.38
3.973E-01	122.34	1.934E-01	123.15
4.608E-01	122.82	1.691E-01	122.86
5.086E-01	123.22	1.447E-01	122.51
5.587E-01	123.65	1.208E-01	122.05
6.083E-01	124.10		
6.590E-01	124.55		
7.083E-01	125.02		
7.788E-01	123.87		
8.091E-01	123.86		
8.608E-01	124.26		
9.093E-01	124.52		
9.578E-01	124.94		
9.800E-01	125.19		
9.945E-01	125.34		
3.892E-04	22.10		
6.040E-04	45.76		
1.290E-03	64.46		
3.760E-03	83.11		
1.484E-02	100.67		
9.645E-01	125.37		

APPENDIX B

Hydrolysis assays

Preparation of solutions for hydrolysis assays

1. Tris buffer solution (Tris HCl)

1M Tris buffer, pH 8.0

Tris base	121	g
Distilled water	800	ml

Tris base was dissolved and pH was adjusted to 8 with HCl. Then, solution was adjusted to 1L with distilled water. Tris buffer solution was later sterile at 121 ^{o}C, pressure 15psi for 15 min. The buffer solution was kept at 4^{o}C

50mM Tris buffer, pH 8.0

1 M Tris buffer, pH 8.0	25	ml
Distilled water	475	ml

Buffer solution was kept at 4^{o}C

2. *p*-Nitrophenyl palmitate solution

p-nitrophenyl palmitate	50	mg
Absolute ethanol	10	ml

p-Nitrophenyl palmitate was dissolved with absolute ethanol. Then, the solution was mixed well and kept in the brown bottle.

Remark: This solution was prepared before use.

ศูนย์วิทยทรัพยากร
จุฬาลงกรณ์มหาวิทยาลัย

APPENDIX C

Calculation of the lipase activity

1. Calculation of enzyme immobilization [36]

The efficiency of immobilization was evaluated in terms of lipase activity, specific activity, protein loading and activity yields as follows:

$$A_{410} = \varepsilon_{410} bc \qquad \text{Equation C 1.1}$$

Where

A_{410} = Absorbance at 410 nm

ε_{410} = Molar extinction coefficient of *p*-nitrophenol at 410 nm

= 15,000 M^{-1} cm^{-1}

b = 1 cm

c = Concentration of *p*-nitrophenyl palmitate

One unit (1 U) was defined as that amount of enzyme that liberated 1 μmol of *p*-NPP per minute under the test conditions. Lipase activity was calculated from

$$\text{Lipase activity (U/g-support)} = \frac{\text{Activity of immobilized lipase}}{\text{Amount of immobilized lipase}}$$

$$\text{Specific activity (U/mg-protein)} = \frac{\text{Activity of immobilize lipase}}{\text{Amount of protein loading}}$$

$$\text{Protein loading yield (\%)} = \frac{\text{Amount of protein loading}}{\text{Amount of protein introduced}} \times 100$$

$$\text{Activity yield (\%)} = \frac{\text{Specific activity of immobilized lipase}}{\text{Specific activity of free lipase}} \times 100$$

APPENDIX D

Protein determination

1. Preparation of solutions for protein assays

The assay reagent is prepared by diluting 1 volume of the dye stock with 4 volumes of distilled H_2O. Then solution was filtered by filter paper, Whatman No. 1. The solution should appear brown, and have a pH of 1.1. It is stable for 4 weeks in a brown bottle at 4°C.

2. Standard curve of BSA

Protein standards should be prepared in the same buffer as the samples to be assayed. A convenient standard curve can be made using bovine serum albumin (BSA) with concentrations of 0.1, 0.2, 0.3, 0.4, 0.5 and 0.6 mg/ml. The method is as follows;

1. Prepare stock bovine serum albumin with concentration 20 mg/ml.
2. 20 mg/ml BSA was diluted with distilled water as 0.1-0.6 mg/ml (Table C-1)

Table D-1 Composition for standard BSA

BSA (mg)	Reagent volume (µl)	
	stock of BSA	dH_2O
0	-	1000
0.1	5	995
0.2	10	990
0.3	15	985
0.4	20	980
0.5	25	975
0.6	30	970

2. Pipet 5 µl of each standard from stock solution was into 96 wells microplate. Protein solutions are normally assayed in duplicate.

3. Add 300 µl of diluted dye reagent to each well and incubated at room temperature for 5 minutes.

4. The product was measured by an increase in the absorbance at 595 nm with micro plate reader.

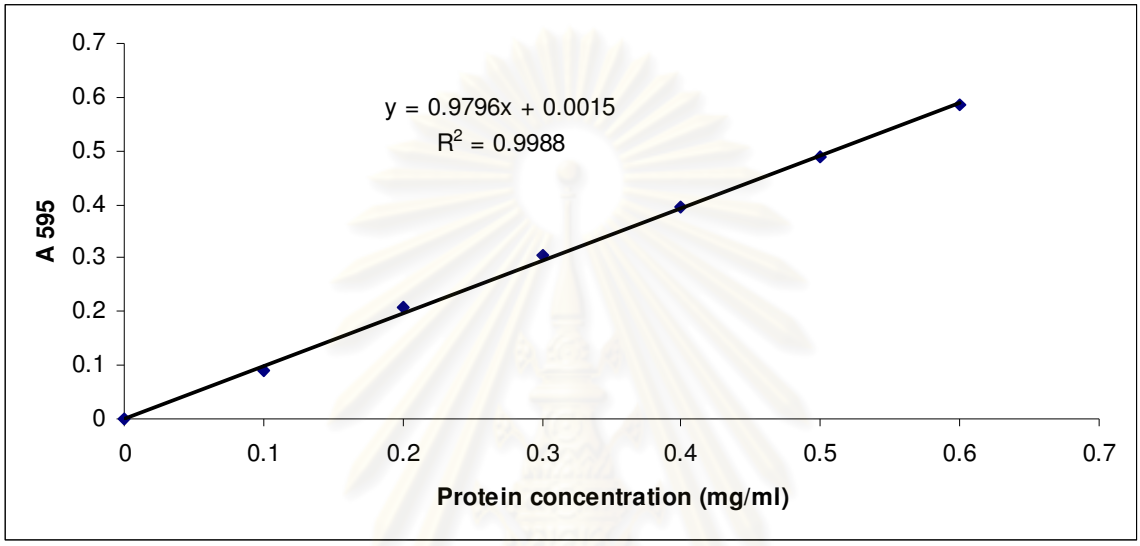

Figure D-1. Calibration curve for protein determination by Bradford's method

3. Calculation of total protein

The absorbance value at 595 nm was calculated by:

$$Y = aX + b$$

Where

Value X axis = Standard protein concentration (mg/ml)

Value Y axis = Absorbance at 595 nm

The amount of bound protein on the support was calculated from the difference between the amount of protein introduced into the reaction mixture and the amount of protein present in the filtrate and washing solutions after immobilization. Amount of bound enzyme onto support (mg/g) was calculated from the following formula:

$$p = \frac{C_i V_i - (C_f V_f + C_w V_w)}{m_s}$$

p = Amount of bound enzyme onto support (mg/g)

C_i = Initial protein concentration (mg/ml)

C_f = Protein concentration of filtrate (mg/ml)

C_w= Protein concentration of washing solution (mg/ml)

V_i = Initial volume of enzyme solution (ml)

V_f = Volume of filtrate (ml)

V_w = Volume of washing solution (ml)

m_s = Weight of the support (g)

ศูนย์วิทยทรัพยากร
จุฬาลงกรณ์มหาวิทยาลัย

BIOGRAPHY

Mr. Bordin Luangon was born on March, 1985 in Nakhon Ratchasima, Thailand. He graduated with the Bachelor Degree of Science in Chemical Technology from Department of Chemical Technology, Faculty of Science, Chulalongkorn University in 2007 and furthered his Master's Degree of Engineering in Chemical Engineering Program, Department of Chemical Engineering, Faculty of Engineering, Chulalongkorn University.

During postgraduate studies, his work has been continuously presented in the international level. The first presentation was presentation at 7th Eco-Energy and Material Science and Engineering Symposium (EMSES 2009) on the topic of "Immobilization of lipase on hierarchical porous carbon monolith" at Chiangmai, Thailand on 19-22 November, 2009. The second was presentation at Pure and Applied Chemistry International Conference (PACCON 2001) on the topic "The optimum condition in lipase immobilization on carbon monolith prepared by continuous process" at Ubon Retchathani, Thailand on 21-23 January, 2010.

ศูนย์วิทยทรัพยากร
จุฬาลงกรณ์มหาวิทยาลัย